

# **A Design Method for a Supersonic Axisymmetric Nozzle for Use in Wind Tunnel Facilities**

a project presented to  
The Faculty of the Department of Aerospace Engineering  
San José State University

in partial fulfillment of the requirements for the degree  
*Master of Science in Aerospace Engineering*

by

**Devyn Yoshio Kapukawai Uyeki**

December 2018

approved by

Dr. Fabrizio Vergine  
Faculty Advisor



## ABSTRACT

### **A DESIGN METHOD OF A SUPERSONIC AXISYMMETRIC NOZZLE FOR USE IN WIND TUNNEL FACILITIES**

by Devyn Yoshio Kapukawai Uyeki

This report provides the theory and methodology used for the design of a supersonic axisymmetric nozzle. This report includes the design of a nozzle to justify the validity of the method discussed. The design approach begins with fundamental, quasi-one-dimensional flow. Then a modified version of the method of characteristics is used to design a shock-free, inviscid, axisymmetric nozzle. The nozzle contour is compared against a previously designed and tested Mach 3, axisymmetric nozzle. A sensitivity analysis is done to determine the range of validity of the method.

Future reports will include inviscid CFD simulations to further verify the design method by ensuring that the nozzle is capable of producing the desired Mach number. Viscous simulations will be performed to determine the boundary layer effects on the nozzle walls. The original inviscid nozzle design is iterated for boundary layer correction and another viscous CFD simulation is done on the final nozzle design to justify that the nozzle is capable of producing the desired flow speed while accounting for boundary layer effects. Finally, the design is presented in as a CAD model.

## Table of Contents

List of Symbols.....	iii
1 Introduction .....	1
1.1 Background.....	1
1.1.1 Introduction to Supersonic Wind Tunnels .....	1
1.1.2 de Laval Nozzle (Convergent-Divergent Nozzle) .....	2
1.1.3 Two-Dimensional Nozzle .....	3
1.1.4 Axisymmetric Nozzle (Three-Dimensional Nozzle) .....	4
1.2 Motivation.....	4
1.2.1 Summary of References .....	4
1.2.2 Importance of Work – Closing the Gap .....	6
1.3 Project Proposal .....	6
1.3.1 Project Goal.....	6
1.3.2 Design Methodology .....	6
2 Reduced Order Model .....	8
2.1 Quasi-One-Dimensional Flow.....	8
2.1.1 Isentropic Flow .....	9
2.1.2 Non-Isentropic Flow.....	11
2.1.3 Expansion Waves.....	12
3 Nozzle Contour Design Method.....	16
3.1 2D Method of Characteristics .....	16
3.1.1 2D Method of Characteristics Implementation.....	18
3.2 Axisymmetric Method of Characteristics - Derivation.....	21
3.3 Axisymmetric Method of Characteristics – Characteristic Point Calculation Procedure .....	24
3.3.1 Step-by-step Procedure to Determine Characteristic Points.....	25
4 Axisymmetric Method of Characteristics Implementation .....	28
4.1 Assumptions .....	28
4.1.1 Initial Nozzle Length.....	28
4.1.2 Axis-Pressure Distribution .....	28
4.2 Inputs .....	30
4.3 Implementation .....	30
4.4 Converging Section Design .....	32
4.5 Axisymmetric MOC Contour.....	32

5	Method Validation.....	34
6	Contour’s Shape Sensitivity Analysis .....	36
6.1	Effects of the Initial Nozzle Length.....	37
6.2	Effects of the Number of Characteristic Lines.....	38
6.3	Results.....	40
	Future Work .....	41
	References .....	42
	Appendices.....	44
	<b>Appendix A: Intersect C Matlab Function .....</b>	<b>45</b>
	<b>Appendix B: AxisMOC Matlab Code .....</b>	<b>47</b>
	<b>Appendix C: Benchmarking Matlab Code .....</b>	<b>55</b>
	<b>Appendix D: Nozzle Contour Coordinates.....</b>	<b>58</b>

## List of Symbols

Symbol	Definition	Units (SI, English)
$a$	Speed of Sound	m/s, ft/s
$A$	Local Cross-Sectional Area	$m^2$ , $in^2$
$A^*$	Throat Area	$m^2$ , $in^2$
$M$	Local Mach Number	-
$M_1$	Mach Number Before Shock	-
$M_2$	Mach Number After Shock	-
$P_b$	Back Pressure	kPa, psi
$P_e$	Exit Pressure	kPa, psi
$P_o$	Total/Reservoir Pressure	kPa, psi
$P_1$	Pressure Before Shock	kPa, psi
$P_2$	Pressure After Shock	kPa, psi
$V_r$	Velocity in Horizontal Direction	m/s, ft/s
	Velocity in Vertical Direction	m/s, ft/s
$w$	Velocity in the Z-Direction	m/s, ft/s
$V$	Local Flow Velocity	m/s, ft/s
$\rho$	Flow Density	$Kg/m^3$ , slug/ft <sup>3</sup>
$\gamma$	Specific Heat Ratio	-

# 1 Introduction

## 1.1 Background

Although World War II officially ended in 1945, there was a great deal of geopolitical tension. This instability amongst the great powers of the world led to the Cold War. Of the world's great powers, the Cold War's core was rooted in a competition of technological superiority between the United States and the Soviet Union. One of the key categories in this competition was space exploration and the space race. This caused the need for high speed launch and re-entry vehicles.

Today, there is a similar space race. However, unlike the Cold War when the race was between government funded international powers, it is now between private companies such as Blue Origin, SpaceX, Orbital Sciences, and Virgin Galactic [1-3]. In order to move forward with a design, various subscale tests must be done. These subscale tests include CFD simulations and wind tunnel testing. While CFD is a powerful tool, results are not always concrete as it requires a high level of user input. Wind tunnels on the other hand, provide a controlled testing environment which results in more realistic subscale model testing to determine aerodynamic characteristics. Engineers then use the subscale data to predict how the full-scale model would perform during its mission.

### 1.1.1 Introduction to Supersonic Wind Tunnels

A supersonic wind tunnel is a facility designed to produce supersonic flows through a test section where experimental tests are conducted and data is collected. Typically, these experiments are done to analyze the flow behavior over subscale models for aircraft and spacecraft. Subscale testing allows engineers to iterate their design before committing funds to a full-scale model.

Two common supersonic wind tunnel configurations include blowdown and suction wind tunnels. Blowdown wind tunnels utilize high pressures upstream of the test section which allows the flow to

accelerate to the desired Mach number through the nozzle. The wind tunnel currently being designed at SJSU is a blow down wind tunnel.

Supersonic wind tunnels consist of five major components. These components are the high-pressure reservoir, plenum, nozzle, test section, and diffuser. Once the wind tunnel runs, air flows from the high-pressure tanks to the plenum. The plenum is used to slow down the flow to subsonic speeds and to accommodate for the pressure variation in the flow. The air accelerates through the nozzle and enters into the test section where the experiment is conducted and data is collected. Finally, the diffuser reduces the speed and pressure of the air before it exits the wind tunnel. For the nozzle to produce a shock-free flow at the desired Mach number, the inlet-to-exit pressure ratio must maintain a certain ratio and needs to be regulated. Since the diffuser reduces the exit pressure, the required inlet pressure is greatly reduced [4-6]. The remainder of this report focuses on the nozzle section. Figure 1.2.1 is a sketch of the five components highlighted above.

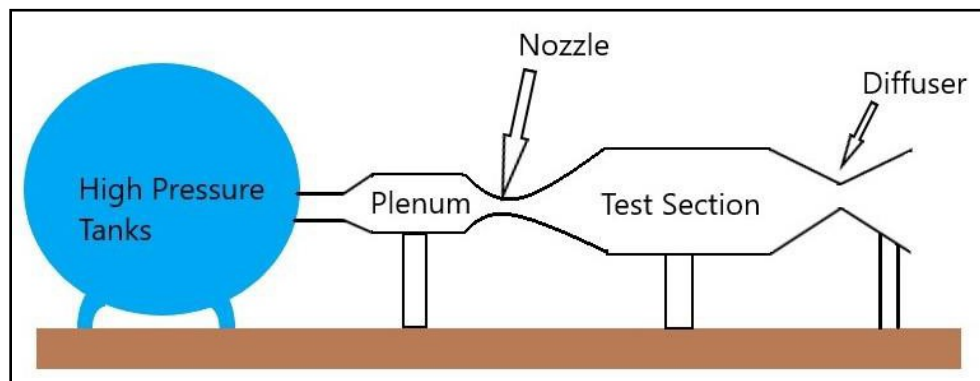


**Figure 1.2.1 – Supersonic Wind Tunnel Schematic**

### 1.1.2 de Laval Nozzle (Convergent-Divergent Nozzle)

A de Laval nozzle, also known as a convergent-divergent (CD) nozzle is composed of three sections: a converging section, throat, and a diverging section. The flow is subsonic ( $M < 1$ ) as it exits the plenum and enters the converging section of the nozzle. Once the flow is in the converging section of the

nozzle, the flow accelerates due to decreasing area. This is justified via conservation of mass flow rate. The flow continues downstream to the throat, where the cross-sectional area is smallest. At the throat of a correctly designed nozzle, the flow is choked ( $M=1$ ). In order for nozzle to reach sonic conditions at the throat, the inlet cross-sectional area to throat area ratio must be a certain value. Additionally, the inlet-to-exit pressure ratio must be a certain value that corresponds to the free stream Mach number. Finally, the flow enters the diverging section where it becomes supersonic ( $M>1$ ) and accelerates to the design Mach number. Like the converging section, the diverging section is also driven by the area and pressure ratios [7-9].

At any given moment while the wind tunnel is running, the exit pressure ( $P_e$ ), may not be equal to the back pressure ( $P_b$ ). Nature corrects this discontinuity through expansion waves and oblique shocks. Thus, one of following scenarios may occur.

- ( $P_e < P_b$ ): Nozzle is overexpanded, oblique shocks form.
- ( $P_e = P_b$ ): Nozzle is perfectly expanded.
- ( $P_e > P_b$ ): Nozzle is under-expanded, expansion waves form.

While a perfectly expanded nozzle is the ideal case, wind tunnels may operate when the nozzle is overexpanded. In the absence of a diffuser, an overexpanded nozzle may still be used to perform experiments and collect data [10].

### 1.1.3 Two-Dimensional Nozzle

A two-dimensional (2D) nozzle is a nozzle that has a rectangular cross section. Traditionally, wind tunnels utilize a 2D nozzle due to the relatively ease of design and manufacturability.

Although 2D nozzles are commonly used in wind tunnel facilities, a major drawback is the uncertainty in the flow caused by the formation of vortices in the corners of the nozzle. While the flow remains uniform within the inviscid core, this uncertainty reduces the size of the area [11].

#### 1.1.4 Axisymmetric Nozzle (Three-Dimensional Nozzle)

An axisymmetric nozzle is a three-dimensional (3D) nozzle. Unlike a 2D nozzle, an axisymmetric nozzle does not have corners which negates the formation of vortices, resulting in a higher quality flow. Although axisymmetric nozzles are not as commonly used in wind tunnel facilities, they are commonly used in rocket propulsion applications.

The unique design of an axisymmetric nozzle for a wind tunnel requires involved mathematics as there is a limited amount of historical data and past research documentation. [12].

## 1.2 Motivation

### 1.2.1 Summary of References

Anderson's *Modern Compressible Flow*, illustrates the differences between the design of a 2D nozzle via method of characteristics (MOC) and the design of an axisymmetric nozzle via MOC. These differences are summarized below.

- The compatibility equations for the design of an axisymmetric nozzle are differential equations while the 2D version's compatibility equations are algebraic.
- The  $(\theta + v)$  quantities along the  $C_+$  and  $C_-$  characteristics for the axisymmetric MOC varies with spatial location while the  $(\theta - v)$  quantities remain constant along the  $C_+$  and  $C_-$  characteristics for the 2D MOC.

Anderson also states that the axisymmetric MOC must be solved with finite differences. It is also states that such techniques are beyond the scope of the book [12].

Rakich's NASA technical note reviews the MOC for 3D supersonic flow. Two methods are discussed: the reference plane method and bicharacteristic method. Additionally, Rakich highlights principle complications that come with the 3D MOC. These complications are summarized below.

- The presence of “cross-derivatives” not along a characteristic in the compatibility equations.
- Interpolation is necessary.

Rakich also explains that these complications are reduced by implementing a reference plane method with a uniform, predefined grid. He also ensures that using this method will produce second-order accuracy. Rakich presents results for flow around inclined circular cones using the methods discussed. The report did not include the implantation of the methods discussed to design an axisymmetric nozzle [13].

Zucrow and Hoffman's *Gas Dynamics* investigates the principle theory behind the MOC. It also includes 2D and axisymmetric applications for the MOC. Examples of numerical methods are also presented. Unfortunately, there was no content covering the application of the MOC for the design of an axisymmetric nozzle [14].

McCabe's report on supersonic nozzle design highlights the design method for supersonic nozzles. The design includes the nozzle's contour to produce a shock-free flow. The report also demonstrates how to calculate the flow inside the nozzle's throat. This report did not include any axisymmetric nozzle design [15].

Hartfield and Burkhalter's conference paper provided a design approach for axisymmetric nozzles via MOC. The conference paper derives the 3D MOC characteristics and compatibility equations from fundamental principles. This procedure is outlined in a concise, step-by-step method. However, the report does not show the procedure used for the implantation of the numerical methods used to

complete the nozzle design via axisymmetric MOC. To complete the design, Hartfield and Burkhalter use a computer solver. Essentially, this report provides an explanation to the fundamental principles behind the nozzle design tool that they used. It did not cover the implantation of these principles while the software ran [12].

### 1.2.2 Importance of Work – Closing the Gap

Although the references reviewed above provide a solid foundation for the MOC, numerical methods, axisymmetric flows, and 2D nozzle design, none of these references provide a complete step-by-step procedure for the design of an axisymmetric nozzle. Since there are supersonic aircraft, rockets, missiles, and a few supersonic wind tunnels that utilize axisymmetric nozzles, a method for axisymmetric nozzle design must already exist. However, the design process is not easily accessible to the public. The purpose of this project is to provide engineers and designers an easily accessible procedure for the design of an axisymmetric supersonic nozzle via MOC. This will be done by implementing numerical methods to the MOC for axisymmetric nozzle design.

## 1.3 Project Proposal

### 1.3.1 Project Goal

The purpose of this report is to present a method to design a supersonic, axisymmetric nozzle for the use in a wind tunnel facility. An example of a nozzle design will also be presented and verified with CFD to justify the design method.

### 1.3.2 Design Methodology

Preliminary analysis on quasi 1-D flow, expansion waves, oblique shocks, supersonic nozzle design and axisymmetric flows must be done before the design process. The methodology used for the design of the axisymmetric nozzle is the following:

1. Analysis on quasi 1-D flow, nozzle and axisymmetric nozzle design and axisymmetric flows.

2. Develop a Matlab code that performs a quasi 1-D study to size the nozzle's exit-to-throat area ratio.
3. Develop a Matlab code that executes an axisymmetric Method of Characteristics to avoid shocks in the nozzle as an initial design of the nozzle's contour.
4. Summarize method used for future nozzle designer's reference.
5. Validate nozzle contour using historical data
6. Perform a sensitivity analysis on key parameters

After the nozzle design is finalized, it will be machined and integrated into the supersonic wind tunnel at SJSU where it will be used for re-entry vehicle research.

## 2 Reduced Order Model

A reduced order model is used as a preliminary design tool to give a prediction of the nozzle's performance in the wind tunnel. A quasi-one-dimensional Matlab program was written to provide a visual representation of the flow conditions. The Matlab program intakes the nozzle geometry and determines the Mach number, temperature ratio, pressure ratio, and any shocks that may occur based off flow conditions. The values are presented graphically while the flow passes through the nozzle. These values are necessary to determine the design envelope for the wind tunnel configuration. Regardless, this reduced order model is not useful for the design of the nozzle's contour to ensure a shock-free flow.

### 2.1 Quasi-One-Dimensional Flow

A quasi-one-dimensional flow (quasi-1D flow) is a flow in which the flow parameters only vary along one direction. A quasi-1D flow analysis yields a top-level design for a nozzle. Mainly, this analysis calculates rough pressure ratios and expansion ratio for the design Mach number. Figure 2.1.1 illustrates a quasi-1D flow through a duct.

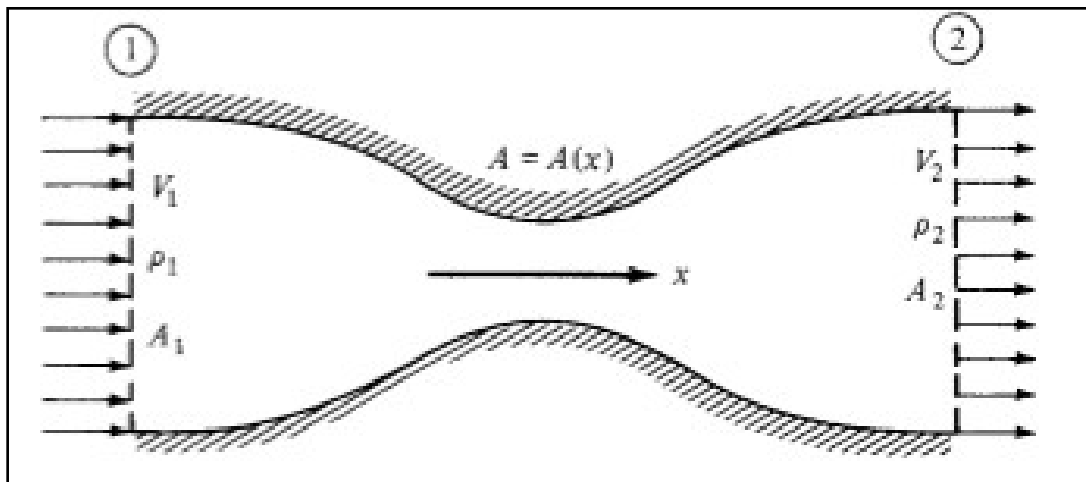


Figure 2.1.1 – Quasi-one-dimensional flow in a duct [17]

### 2.1.1 Isentropic Flow

For the reduced order model, the core flow is assumed to be isentropic. An isentropic flow is the ideal type of flow as it is both adiabatic, meaning no heat addition and inviscid. This assumption may be justified by the following.

- Heat transfer effects between the flow and the nozzle walls are minimal due to short run times of the high-speed flow.
- Reynolds number of the core is much higher than the Reynolds number near the nozzle walls.
  - Due to the characteristic length to the nozzle core being greater.

During experiments, subscale models will be placed in the center of the test section where it will only be under the influence of the isentropic core flow. Figure 2.1.2 illustrates the geometry of a predetermined CD nozzle. This nozzle geometry was used for the quasi-1D calculations and is designed to generate a Mach 3 flow. Based off plenum conditions, a Mach 3 nozzle was selected due to its optimal run time and usable test area of an overexpanded nozzle [18].

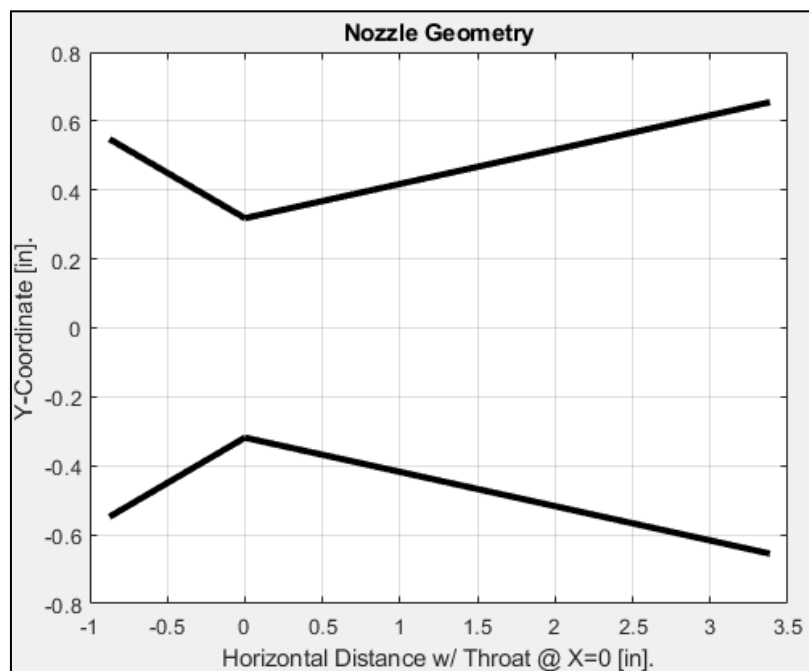


Figure 2.1.2 – Geometry of Predetermined Nozzle.

With the geometry of the nozzle known, the area-Mach relationship presented below is used to determine the Mach number at each location along the nozzle's length. The Matlab code forces the nozzle to choke at the throat and assumes that the specific heat ratio ( $\gamma$ ) is 1.4 (standard for air).

$$\left(\frac{A}{A^*}\right)^2 = \frac{1}{M^2} \left[ \left(\frac{\gamma-1}{\gamma+1}\right) M^2 + \frac{\gamma-1}{2} M^2 \right] \quad (2.1)$$

The area-Mach relationship yields a subsonic and supersonic value for each area ratio. Although the flow is accelerating through the converging section it remains subsonic until it reaches the throat where it chokes. After the throat, the flow enters the diverging section where the pressure ratio between the backpressure and plenum drives the flow to either accelerate to supersonic or decelerate to subsonic. The equation that describes this relationship is shown below.

$$\frac{P}{P_o} = \left(1 + \frac{\gamma-1}{2} M^2\right)^{-\frac{\gamma}{\gamma-1}} \quad (2.2)$$

Finally, there is one last scenario: a fully subsonic solution. Figure 2.1.3 below illustrates the three possible scenarios for the Mach 3 nozzle shown in Figure 2.1.2.

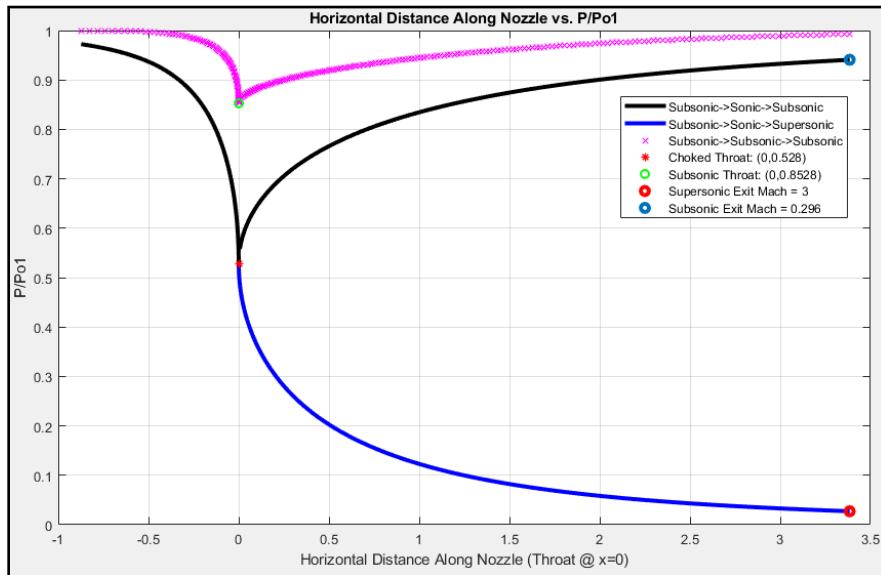


Figure 2.1.3 – Pressure Ratio Driving the Mach Number Throughout the Nozzle.

## 2.1.2 Non-Isentropic Flow

Non-isentropic flows occur when there is a change in entropy within the flow. Nature accommodates for this sharp change with shockwaves. Shockwaves increase the pressure to match the back pressure to be continuous. There are two types of shockwaves that may form: normal or oblique shocks. Normal shocks occur normal to the flow and are the strongest shock wave. Oblique shocks are weaker and are angled to the flow direction.

### 2.1.2.1 Normal Shocks

Across a normal shock, the total pressure suddenly decreases, the pressure ratio increases, and the flow becomes subsonic. Equation 2.3 and 2.4 describes the Mach number relationship and pressure ratio across a normal shock.

$$M_2 = \sqrt{\frac{1 + \frac{\gamma-1}{2} M_1^2}{\gamma M_1^2 - \frac{\gamma-1}{2}}} \quad (2.3)$$

$$\frac{P_o}{P_b} = 1 + \frac{2\gamma}{\gamma+1} (M_1^2 - 1) \quad (2.4)$$

By manipulating equations 2.2 through 2.4, a ratio between the plenum pressure and the back pressure ( $P_o/P_b$ ) is found. This ratio is used to determine if a normal shock will occur within the nozzle and if a normal shock occurs at the nozzle exit.

### 2.1.2.2 Oblique Shocks

Oblique shocks occur when the nozzle is overexpanded. This is when  $P_o/P_b$  is higher than the value required for a normal shock to occur at the nozzle exit but less than the value required for an isentropic flow. Oblique shocks allow the pressure to increase to match the back pressure. Oblique shocks also decrease the Mach number. However, these changes in pressure and Mach number are not as drastic compared to the normal shock. Unlike the normal shock, oblique shocks occur at an angle  $\beta$ , which

often allow the flow to remain supersonic. If the tunnel were to run overexpanded without a test section, oblique shock calculations are necessary to determine the usable area behind the nozzle exit.

### 2.1.3 Expansion Waves

Expansion waves occur when the nozzle is Underexpanded. This is when  $P_o/P_b$  is higher than the value required for the perfectly expanded nozzle. Expansion waves accelerate the flow, increasing the Mach number.

## 2.2 The Matlab Code

The Matlab code uses the isentropic and shock relationships to determine the required plenum pressure to have a perfectly expanded flow and the required plenum pressure to have a normal shock at the exit of the nozzle. Additionally, the Matlab code prompts the user to input a plenum pressure and shows the user if a normal shock, oblique shocks, or expansion waves occur based off the plenum pressure. If a normal shock occurs within the diverging section, the code finds the location of the shock. If the nozzle is overexpanded, the code will determine where the oblique shocks converge behind the nozzle exit. Finally, if the nozzle is Underexpanded, the code will determine what Mach number the flow will expand to. Examples of the non-isentropic scenarios for the same Mach 3 nozzle are presented in Figures 2.2.1 through 2.2.5 below. For the same nozzle, the Matlab code determined that a plenum pressure of 36.7 will yield a perfectly expanded nozzle and for a normal shock to occur at the nozzle exit the plenum pressure must be 3.55 atm.

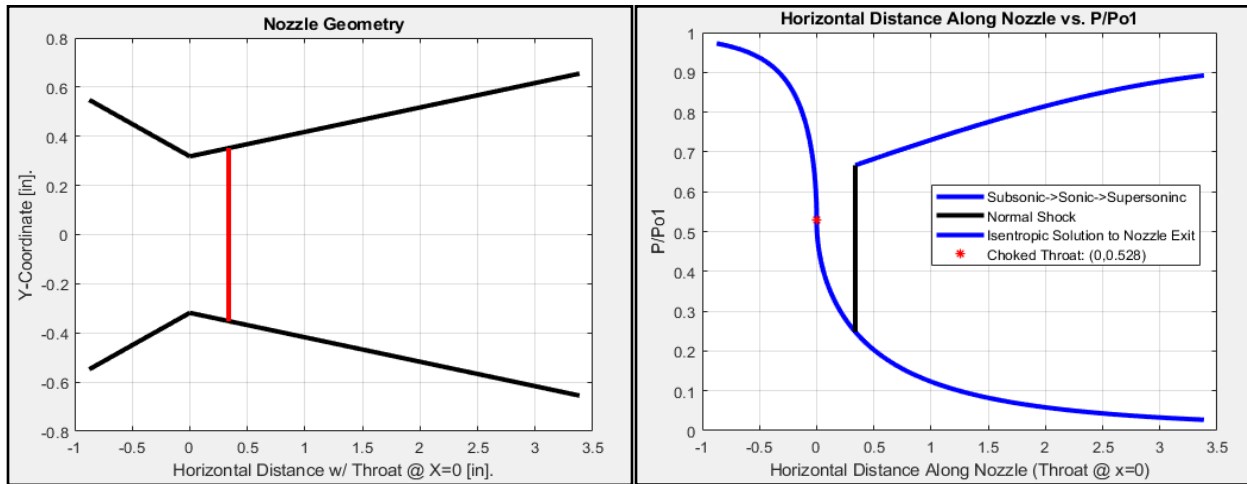


**Figure 2.2.1 – Plenum Pressure of 1.5 atm Causes a Normal Shock to Occur 0.338 inches from Nozzle Throat.**

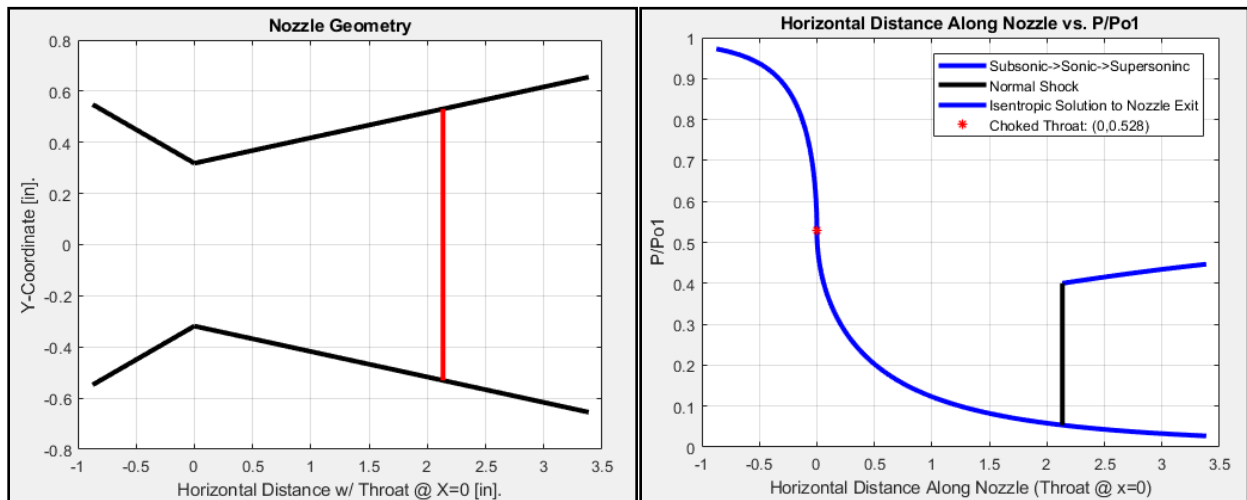


**Figure 2.2.2 – Plenum Pressure of 2.5 atm Causes a Normal Shock to Occur 2.134 inches from Nozzle Throat.**

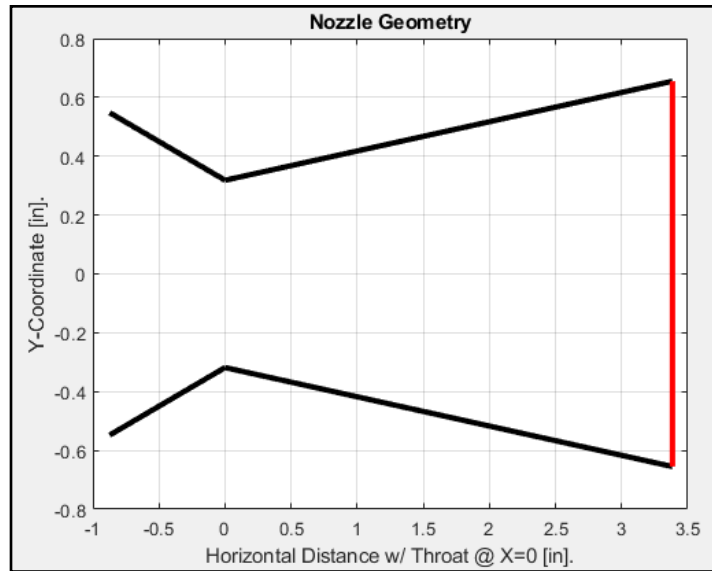


Figure 2.2.3 – Plenum Pressure of 3.55 atm Causes a Normal Shock to Occur at Nozzle Exit.

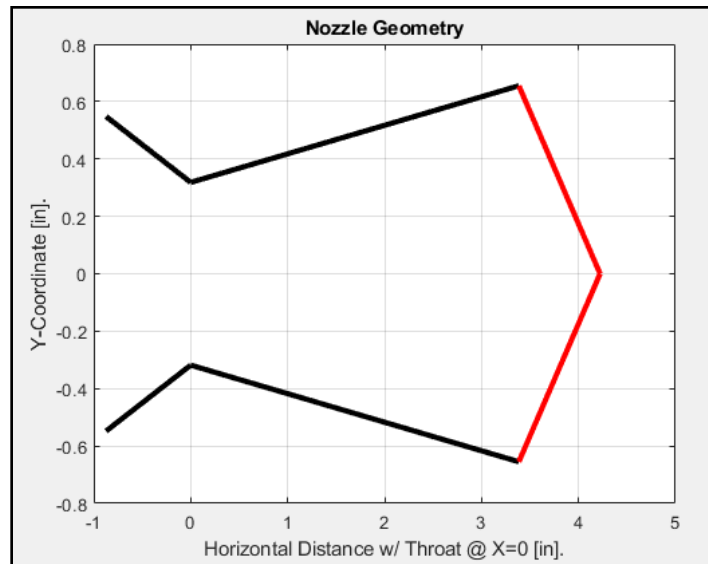
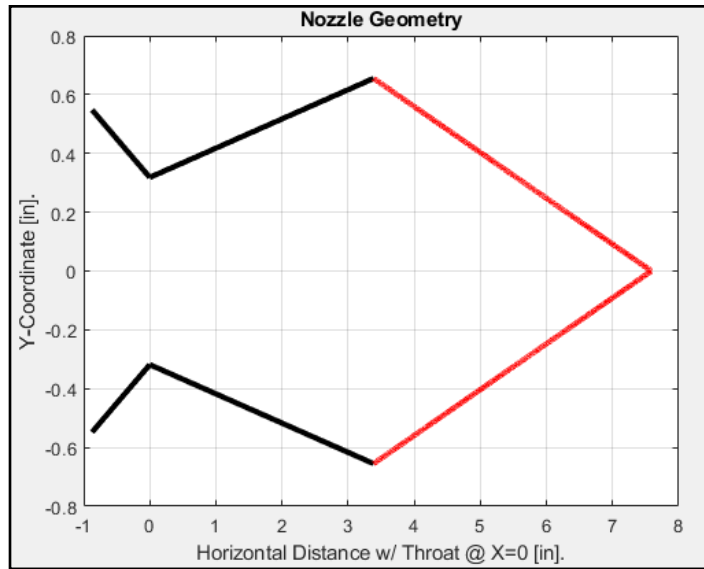


Figure 2.2.4 – Plenum Pressure of 4.5 atm Causes Oblique Shocks to Occur. The Shocks Converge 0.838 inches from the Nozzle Exit.



**Figure 2.2.5 – Plenum Pressure of 30 atm Causes Oblique Shocks to Occur. The Shocks Converge 4.20 inches from the Nozzle Exit.**

### 3 Nozzle Contour Design Method

While the importance of the reduced order model covered in the previous chapter cannot be overlooked, the quasi-1D flow analysis is not useful for the design of the nozzle's contour. It is necessary that nozzle's contour is designed in a fashion that allows for a shock-free expansion. To do this, a modified version of the 2D method of characteristics is used to produce the desired supersonic, axisymmetric flow. For the remainder of this report this method will be referred to as the axisymmetric MOC.

#### 3.1 2D Method of Characteristics

This section highlights the 2D MOC procedure used to design a Mach 3, 2D nozzle contour. The 2D MOC provides a solid foundation to the visual understanding of the 3D method to be developed in chapter 4.

A 2D nozzle is designed via MOC. The 2D MOC is derived from the governing equation for a 2D, steady, adiabatic, irrotational flow.

$$\left(1 - \frac{u^2}{a^2}\right) \frac{\delta^2 \phi}{\delta x^2} + \left(1 - \frac{v^2}{a^2}\right) \frac{\delta^2 \phi}{\delta y^2} - \frac{2uv}{a^2} \frac{\delta^2 \phi}{\delta x \delta y} = 0 \quad (3.1)$$

Substituting in velocity potential terms and differentiating yields equations 3.2 through 3.4.

$$\left(1 - \frac{u^2}{a^2}\right) \frac{\delta^2 \phi}{\delta x^2} + \left(1 - \frac{v^2}{a^2}\right) \frac{\delta^2 \phi}{\delta y^2} - \frac{2uv}{a^2} \frac{\delta^2 \phi}{\delta x \delta y} = 0 \quad (3.2)$$

$$du = \frac{\delta^2 \phi}{\delta x^2} dx + \frac{\delta^2 \phi}{\delta x \delta y} dy \quad (3.3)$$

$$dv = \frac{\delta^2 \phi}{\delta x \delta y} dx + \frac{\delta^2 \phi}{\delta y^2} dy \quad (3.4)$$

The step by step derivation of equations 3.2 through 3.4 can be found in reference 11. These equations can be used as a system of equations to solve for  $\frac{\delta^2 \phi}{\delta x \delta y}$  using Cramer's rule shown in equation 3.5.

$$\frac{\delta^2\phi}{\delta x\delta y} = \frac{\begin{vmatrix} 1-\frac{u^2}{a^2} & 0 & 1-\frac{v^2}{a^2} \\ \frac{du}{dx} & \frac{dv}{dy} & 0 \end{vmatrix}}{\begin{vmatrix} 1-\frac{u^2}{a^2} & -\frac{2uv}{a^2} & 1-\frac{v^2}{a^2} \\ \frac{du}{dx} & \frac{dv}{dy} & 0 \end{vmatrix}} \quad (3.5)$$

Where  $\frac{\delta^2\phi}{\delta x\delta y}$  is indeterminate along the characteristic line when the numerator and denominator is set to zero in equation 3.5. Furthermore, the direction of the characteristic lines is found by setting the denominator to zero and solving for  $\frac{dy}{dx}$ . This yields equation 3.6 below.

$$\left(\frac{dy}{dx}\right)_{char} = \frac{-\frac{uv}{a^2} \pm \sqrt{\left[\frac{u^2+v^2}{a^2}\right]-1}}{1-\left(\frac{u^2}{a^2}\right)} \quad (3.6)$$

Equation 3.6 is further simplified by substituting the speed of sound with the local Mach angle  $\mu$  with  $V\cos\theta$  and  $v$  with  $V\sin\theta$ . This relationship is shown below in equation 3.7.

$$\left(\frac{dy}{dx}\right)_{char} = \tan(\theta \mp \mu) \quad (3.7)$$

Equation 3.7 shows that any given point within the nozzle, can be defined by the intersection of two characteristic lines. These characteristic lines are referred to as a left-running ( $C_+$ ) characteristic and a right-running ( $C_-$ ) characteristic. Once the characteristic lines are found, the compatibility equations that hold true along the characteristic lines are found by setting the numerator to zero. This is shown below in equation 3.8.

$$\frac{dv}{du} = -\frac{\left(1-\frac{u^2}{a^2}\right)}{\left(1-\frac{v^2}{a^2}\right)} \frac{dy}{dx} \quad (3.8)$$

Substituting equation 3.6 into 3.8 yields equation 3.9 shown below.

$$\frac{dv}{du} = \frac{uv}{a^2} \mp \frac{\sqrt{u^2+v^2}-1}{\left(1-\frac{v^2}{a^2}\right)} \quad (3.9)$$

After substituting  $u = V\cos\theta$  and  $v$  with  $V\sin\theta$  and algebraic manipulation, equation 3.9 becomes equations 3.10. Additionally, integrating equation 3.9 yields the Prandtl-Meyer function applied as an algebraic expression shown in equation 3.11 and 3.12.

$$d\theta = \mp \sqrt{M^2-1} \frac{dv}{v} \quad (3.10)$$

$$\theta + \nu(M) = K_- \quad (3.11)$$

$$\theta - \nu(M) = K_+ \quad (3.12)$$

Equations 3.2 and 3.3 state that the  $K_-$  and  $K_+$  values along any  $C_-$  and  $C_+$  characteristic is constant. Hence, once the  $K_-$  or  $K_+$  value is known at any given point, that value will remain constant along the respective characteristic line.

### 3.1.1 2D Method of Characteristics Implementation

This section contains an example of the process used to design a minimum length, 2D, Mach 3 nozzle. For this example, seven characteristic lines are used. It should be noted that there are an infinite number of characteristic lines and that the use of more characteristic lines correlates to higher accuracy. Regardless, the purpose of this section is to show the implantation of the 2D MOC, thus the goal of this example is to design a contour that is within a ten percent error margin of the quasi-1D calculations.

The nozzle throat height is a preset value of 0.9445 inches. Thus, from the centerline, the distance is 0.472 inches. This value was selected based off constraints set by optimizing plenum pressure, exit area, and a constant depth of 4 inches throughout the expansion section. The seven characteristic lines start at the throat to form a simple expansion. These characteristics extend to and reflect off the

nozzle centerline. This configuration yields a total of 35 points. Figure 3.1.1 is schematic showing the characteristic lines.

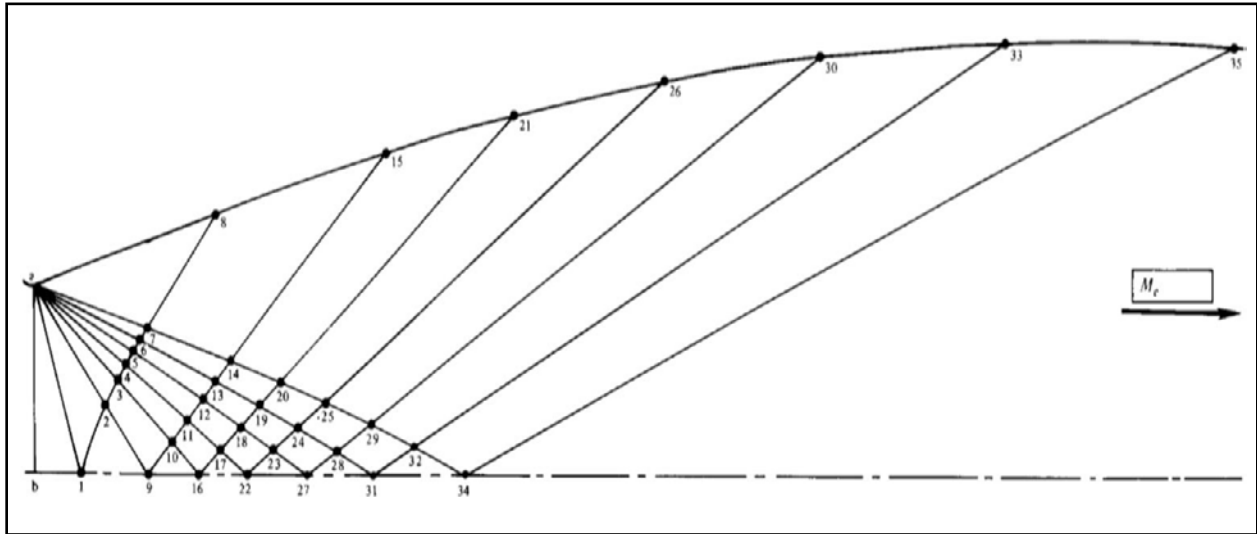


**Figure 3.1.1: Schematic of Seven Characteristic Lines [11]**

The Prandtl Meyer angle ( $\nu$ ) that corresponds to Mach 3 is 49.76 degrees. Half of this value yields the highest  $\theta$  value for the nozzle contour. This angle is formed with the line between points a and 8 with the horizontal. Once this angle is found, the angles of points one through nine are found by a constant change in  $\theta$ . After these initial steps are done, the properties of the remaining points are found using equations 3.1 through 3.3. Table 3.1 summarizes the properties of each point within the web of characteristic lines.

Table 3.1: Seven Line MOC for a Mach 3 Nozzle. Wall points are highlighted.

Point #	$k^- = \theta + \nu$	$k^+ = \theta - \nu$	$\theta = 1/2(k^- + k^+)$	$\nu = 1/2(k^- - k^+)$	M	$\mu$	$\theta + \mu$ & Wall Inclination	$\theta - \mu$	x	y
a	0.004	0	0.002	0.002	1.001	87.215	24.88		0	0.472
1	1.76	0	0.88	0.88	1.0749	68.4827	69.3627	-68.4827	0.18609	0
2	9.76	0	4.88	4.88	1.2519	53.0136	57.8936	-53.0136	0.24256	0.14995
3	17.76	0	8.88	8.88	1.3963	45.7406	54.6206	-45.7406	0.27048	0.19444
4	25.76	0	12.88	12.88	1.533	40.7151	53.5951	-40.7151	0.29022	0.22224
5	33.76	0	16.88	16.88	1.6684	36.8256	53.7056	-36.8256	0.3056	0.24314
6	41.76	0	20.88	20.88	1.8054	33.6354	54.5154	-33.6354	0.31823	0.26029
7	49.76	0	24.88	24.88	1.946	30.9224	55.8024	-30.9224	0.32876	0.27507
8	49.76	0	24.88	24.88	1.946	30.9224	22.44		0.67545	0.78525
9	9.76	-9.76	0	9.76	1.4267	44.4999	44.4999	-44.4999	0.39515	0
10	17.76	-9.76	4	13.76	1.5628	39.7824	43.7824	-35.7824	0.45654	0.06033
11	25.76	-9.76	8	17.76	1.6983	36.0736	44.0736	-28.0736	0.50561	0.10736
12	33.76	-9.76	12	21.76	1.4954	33.0031	45.0031	-21.0031	0.54926	0.14961
13	41.76	-9.76	16	25.76	1.9776	30.3756	46.3756	-14.3756	0.59022	0.19058
14	49.76	-9.76	20	29.76	2.1249	28.0745	48.0745	-8.0745	0.63001	0.23233
15	49.76	-9.76	20	29.76	2.1249	28.0745	18		1.39251	1.08138
16	17.76	-17.76	0	17.76	1.4954	36.0736	36.0736	-36.0736	0.53936	0
17	25.76	-17.76	4	21.76	1.8359	33.0031	37.0031	-29.0031	0.60846	0.05034
18	33.76	-17.76	8	25.76	1.9776	30.3756	38.3756	-22.3756	0.67273	0.09878
19	41.76	-17.76	12	29.76	2.1249	28.0745	40.0745	-16.0745	0.73571	0.14865
20	49.76	-17.76	16	33.76	2.2792	26.0239	42.0239	-10.0239	0.79955	0.20236
21	49.76	-17.76	16	33.76	2.2792	26.0239	14		1.99064	1.27573
22	25.76	-25.76	0	25.76	1.9776	30.3756	30.3756	-30.3756	0.69435	0
23	33.76	-25.76	4	29.76	2.1249	28.0745	32.0745	-24.0745	0.78063	0.05057
24	41.76	-25.76	8	33.76	2.2792	26.0239	34.0239	-18.0239	0.86829	0.10551
25	49.76	-25.76	12	37.76	2.4422	24.1714	36.1714	-12.1714	0.96037	0.16767
26	49.76	-25.76	12	37.76	2.4422	24.1714	10		2.72706	1.45934
27	33.76	-33.76	0	33.76	2.2792	26.0239	26.0239	-26.0239	0.88421	0
28	41.76	-33.76	4	37.76	2.4422	24.1714	28.1714	-24.1714	0.98918	0.05125
29	49.76	-33.76	8	41.76	2.6154	22.4794	30.4794	-22.4794	1.09926	0.1102
30	49.76	-33.76	8	41.76	2.6154	22.4794	6		3.67572	1.62661
31	41.76	-41.76	0	41.76	2.6154	22.4794	22.4794	-22.4794	1.11305	0
32	49.76	-41.76	4	45.76	2.8007	20.9195	24.9195	-16.9195	1.2607	0.0611
33	49.76	-41.76	4	45.76	2.8007	20.9195	2		4.9094	1.75628
34	49.76	-49.76	0	49.76	3	19.47	19.47	-19.47	1.43351	0
35	49.76	-49.76	0	49.76	3	19.47	0		6.56487	1.81409

Execution of the 2D MOC for a Mach 3 nozzle with seven characteristic lines provided decent results. The quasi-1D expansion ratio was calculated to be 4.235 while the 2D MOC yielded a value of 3.843. The percent error for this design is 9.24% which is within the ten percent margin desired to justify the method. The design of this nozzle is shown in figure 3.1.2. This figure was produced in Solidworks by following the characteristic web and plotting each line at the specified angles listed in Table 3.1, columns eight and nine ( $\theta + \mu$ ) and ( $\theta - \mu$ ).

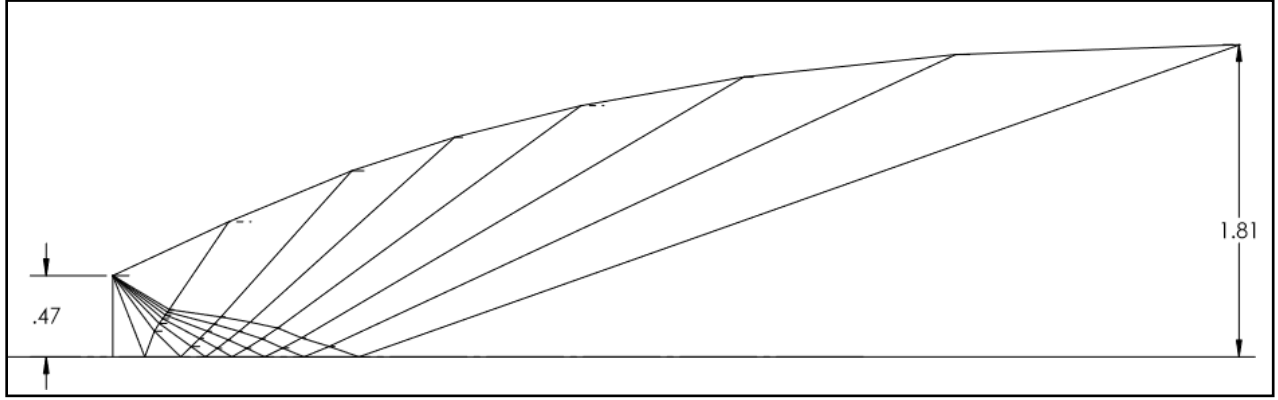


**Figure 3.1.2: Seven Line MOC for a Mach 3 Nozzle.**

### 3.2 Axisymmetric Method of Characteristics - Derivation

The axisymmetric method of characteristics is an iterative method used for designing an axisymmetric nozzle. The nozzle contour is designed by locating and solving for characteristic lines. Although this method is similar to the 2D MOC, slight differences in the compatibility equations cause for an iterative process. Additionally, the axisymmetric MOC requires multiple assumptions and inputs to yield a successful nozzle design covered in section four. To justify convergence, the expansion ratio is iterated over and checked against the quasi-1D value.

$$\frac{\partial(\rho u)}{\partial x} + \frac{\partial(\rho v)}{\partial r} + \frac{1}{r} \frac{\partial(\rho w)}{\partial \phi} + \frac{\rho v}{r} = 0 \quad (3.13)$$

Accounting for steady, inviscid, axisymmetric, irrotational, flow, equation 3.13 yields

$$\left(1 - \frac{u^2}{a^2}\right) \frac{\partial u}{\partial x} - 2 \frac{uv}{a^2} \frac{\partial v}{\partial x} + \left(1 - \frac{v^2}{a^2}\right) \frac{\partial v}{\partial r} = -\frac{v}{r} \quad (3.14)$$

$$du = \frac{\partial u}{\partial x} dx + \frac{\partial v}{\partial x} dr \quad (3.15)$$

$$dv = \frac{\partial v}{\partial x} dx + \frac{\partial v}{\partial r} dr \quad (3.16)$$

The step by step derivation of equations 3.2 through 3.4 can be found in reference 11. These equations can be used as a system of equations to solve for  $\frac{\partial v}{\partial x}$  using Cramer's rule shown in equation 3.15.

$$\frac{\partial v}{\partial x} = \frac{\begin{vmatrix} u^2 & v & -\frac{v^2}{a^2} \\ 1-\frac{u^2}{a^2} & -\frac{v}{r} & 1-\frac{v^2}{a^2} \\ \frac{dv}{dx} & \frac{dr}{du} & 0 \end{vmatrix}}{\begin{vmatrix} 1-\frac{u^2}{a^2} & -\frac{2uv}{a^2} & 1-\frac{v^2}{a^2} \\ \frac{dv}{dx} & \frac{dr}{dr} & 0 \\ 0 & \frac{dx}{dx} & \frac{dr}{dr} \end{vmatrix}} \quad (3.15)$$

Similar to the 2D MOC, the direction of the characteristic lines is found by setting the denominator to zero and solving for  $\frac{dr}{dx}$ . This yields equation 3.16 below.

$$\left(\frac{dr}{dx}\right)_{char} = \frac{-\frac{uv \pm \sqrt{[u^2+v^2]-1}}{a^2}}{1-\left(\frac{v^2}{a^2}\right)} \quad (3.16)$$

Equation 3.6 is further simplified by substituting the speed of sound with the local Mach angle  $\mu$  with  $V \cos \theta$  and  $v$  with  $V \sin \theta$ . This simplification shows that for an axisymmetric flow, the characteristic lines are Mach lines and that the left-running  $C_+$  characteristic and right-running  $C_-$  characteristic are the same as the 2D case. This relationship is shown below in equation 3.17.

$$\left(\frac{dr}{dx}\right)_{char} = \tan(\theta \mp \mu) \quad (3.17)$$

Once the characteristic lines are found, the compatibility equations that hold true along the characteristic lines are found by setting the numerator to zero. This is shown below in equation 3.18.

$$\frac{dv}{du} = -\frac{\left(1-\frac{u^2}{a^2}\right)}{\left(1-\frac{v^2}{a^2}\right)} \frac{dr}{dx} - \frac{\frac{v dr}{r du}}{\left(1-\frac{v^2}{a^2}\right)} \quad (3.18)$$

Substituting equation 3.16 into 3.18 yields equation 3.19 shown below.

$$\frac{dv}{du} = \frac{uv}{a^2} \mp \frac{\sqrt{u^2+v^2}-1}{(1-\frac{v^2}{a^2})} - \frac{v dr}{(1-\frac{v^2}{a^2})} \quad (3.19)$$

After substituting  $u = V \cos \theta$  and  $v$  with  $V \sin \theta$  and algebraic manipulation, equation 3.19 becomes equations 3.20 and 3.21.

$$d(\theta + \nu) = \frac{1}{\sqrt{M^2-1-\cot\theta}} \frac{dr}{r}, \text{ along a } C_- \text{ characteristic.} \quad (3.20)$$

$$d(\theta - \nu) = \frac{-1}{\sqrt{M^2-1+\cot\theta}} \frac{dr}{r}, \text{ along a } C_+ \text{ characteristic.} \quad (3.21)$$

For an axisymmetric, irrotational flow, equations 3.20 and 3.21 are the compatibility equations. Guentert and Neumann presented in reference 19, group the compatibility and characteristic equations into two groups for application purposes. These two groups are presented below in equations 3.22 through 3.25.

First group:

$$\left(\frac{dr}{dx}\right)_1 = \tan(\theta + \mu) \quad (3.22)$$

$$\frac{dV}{V} - \tan(\mu) d\theta - \frac{\tan(\mu) \sin(\mu) \sin(\theta)}{\cos(\theta+\mu)} \frac{dx}{r} = 0 \quad (3.23)$$

Second group:

$$\left(\frac{dr}{dx}\right)_2 = \tan(\theta - \mu) \quad (3.24)$$

$$\frac{dV}{V} + \tan(\mu) d\theta - \frac{\tan(\mu) \sin(\mu) \sin(\theta)}{\cos(\theta-\mu)} \frac{dx}{r} = 0 \quad (3.25)$$

Figure 3.1.1 offers an illustration of these two groups.

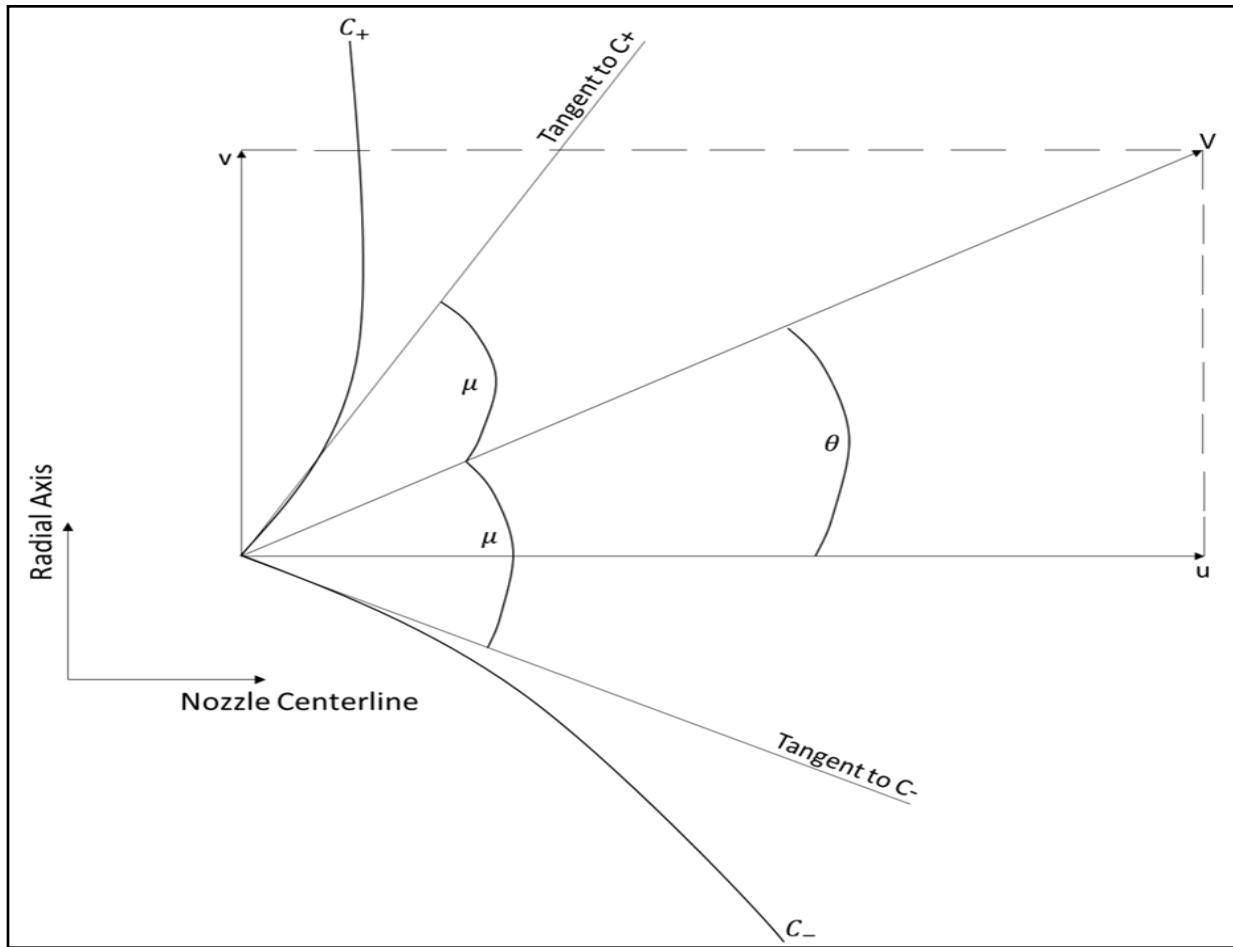


**Figure 3.2.1** - Characteristic lines and velocity vectors of an arbitrary point in the flow.

### 3.3 Axisymmetric Method of Characteristics – Characteristic Point Calculation Procedure

In order to design the nozzle's contour using the equations derived in the previous section, finite differences and an iterative process is required. This section outlines the procedure used to locate and calculate the flow properties at various points throughout the flow field. Figure 3.2.1 serves as visual clarification for the procedure outlined below.

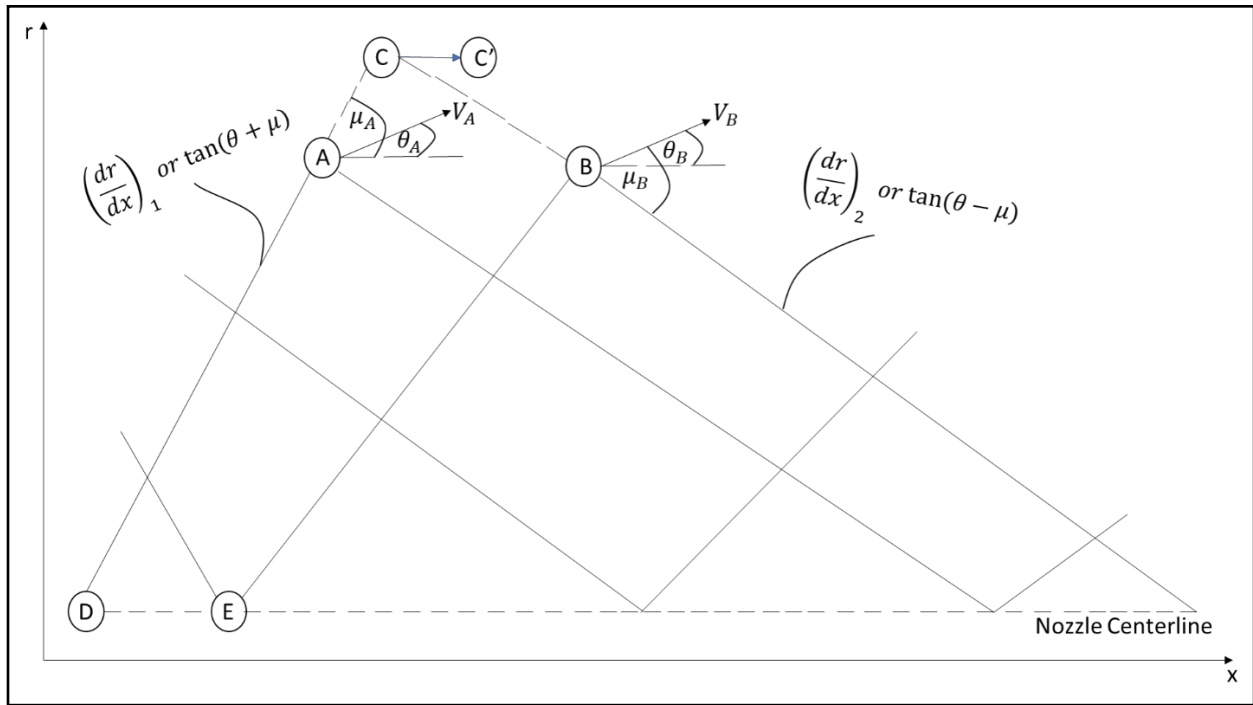


**Figure 3.2.2 – Reference for Axisymmetric MOC Procedure**

### 3.3.1 Step-by-step Procedure to Determine Characteristic Points

This section highlights the iterative method developed that is used to determine individual points within the web of intersecting characteristic lines.

1. Assume properties at points A and B are known and the distance between these points is small. Since the properties are known and small, discretization can be used transform differential terms via finite differences. For example, given two arbitrary points 1 and 2,  $dr/dx$  is transformed in to  $\frac{r_2 - r_1}{x_2 - x_1}$ .
2. Point C is the intersection of the characteristics ie:  $\tan(\theta_B - \mu_B)$  and  $\tan(\theta_A + \mu_A)$
3. Solve for the location of point C ( $x_C, r_C$ ) with finite differences.

$$\frac{r_C - r_A}{x_C - x_A} = \tan(\theta_A + \mu_A) \quad (3.26)$$

$$\frac{r_C - r_B}{x_C - x_B} = \tan(\theta_B - \mu_B) \quad (3.27)$$

Solving for the system of equations yield equations 3.18 and 3.19.

$$x_C = \frac{r_A - r_B + x_B \tan(\theta_B - \mu_B) - x_A \tan(\theta_A + \mu_A)}{\tan(\theta_B - \mu_B) - \tan(\theta_A + \mu_A)} \quad (3.28)$$

$$r_C = r_A + (x_C - x_A) \tan(\theta_A + \mu_A) \quad (3.29)$$

4. Solve for  $V_C$  and  $\theta_C$  with finite differences.

$$\frac{V_C - V_A}{V_A} - (\theta_C - \theta_A) \tan \mu_A - \frac{\tan \mu_A \sin \mu_A \sin \theta_A (x_C - x_A)}{\cos(\theta_A + \mu_A) r_A} = 0 \quad (3.30)$$

$$\frac{V_C - V_B}{V_B} + (\theta_C - \theta_B) \tan \mu_B - \frac{\tan \mu_B \sin \mu_B \sin \theta_B (x_C - x_B)}{\cos(\theta_B - \mu_B) r_B} = 0 \quad (3.31)$$

Solving for the system of equations yields equations 3.22 and 3.23.

$$V_C = \frac{1}{\frac{\cot \mu_A}{V_A} + \frac{\cot \mu_B}{V_B}} \left[ \cot \mu_A \left( 1 + \frac{\tan \mu_A \sin \mu_A \sin \theta_A (x_C - x_A)}{r_A \cos(\theta_A + \mu_A)} \right) + \cot \mu_B \left( 1 + \frac{\tan \mu_B \sin \mu_B \sin \theta_B (x_C - x_B)}{r_B \cos(\theta_B - \mu_B)} \right) + \theta_B - \theta_A \right] \quad (3.32)$$

$$\theta_C = \theta_A + \cot \mu_A \left[ \frac{V_C - V_A}{V_A} - \frac{\tan \mu_A \sin \mu_A \sin \theta_A (x_C - x_A)}{r_A \cos(\theta_A + \mu_A)} \right] \quad (3.33)$$

5. Calculate the speed of sound at point C to determine the Mach angle at point C.

6. Since the properties of point C were found by assuming the properties at points A and B,

a second iteration is required. This is done by averaging points A & C, and C & B. The second

iteration of point C is called C'.

7. Solve for the location of point C' ( $x_C'$ ,  $r_C'$ ).

$$x_C' = \frac{r_A - r_B + \frac{1}{2} [\tan(\theta_B - \mu_B) + \tan(\theta_C - \mu_C)] x_B - \frac{1}{2} [\tan(\theta_A + \mu_A) + \tan(\theta_C + \mu_C)] x_A}{\frac{1}{2} [\tan(\theta_B - \mu_B) + \tan(\theta_C - \mu_C) - \tan(\theta_A + \mu_A) - \tan(\theta_C + \mu_C)]} \quad (3.34)$$

$$r'_C = r_A + (x_C - x_A) \frac{1}{2} [\tan(\theta_A + \mu_A) + \tan(\theta_C + \mu_C)] \quad (3.35)$$

8. Solve for  $V_C'$  and  $\theta_C'$  in a similar fashion.

$$V'_C = \frac{1}{4[(V_A + V_C)^{-1}(\tan\mu_A + \tan\mu_C)^{-1} + (V_B + V_C)^{-1}(\tan\mu_B + \tan\mu_C)^{-1}]^*}$$

$$\frac{2}{\tan\mu_A + \tan\mu_C} \left[ \frac{2V_A}{V_A + V_C} + \frac{\frac{\tan\mu_A \sin\mu_A \sin\theta_A}{r_A \cos(\theta_A + \mu_A)} + \frac{\tan\mu_C \sin\mu_C \sin\theta_C}{r_C \cos(\theta_C + \mu_C)}}{2} (x_C - x_A) \right]$$

$$+ \frac{2}{\tan\mu_B + \tan\mu_C} \left[ \frac{2V_B}{V_B + V_C} + \frac{\frac{\tan\mu_B \sin\mu_B \sin\theta_B}{r_B \cos(\theta_B - \mu_B)} + \frac{\tan\mu_C \sin\mu_C \sin\theta_C}{r_C \cos(\theta_C - \mu_C)}}{2} (x_C - x_B) \right] + \theta_B - \theta_A \quad (3.36)$$

$$\theta'_C = \theta_A + \frac{2}{\tan\mu_A + \tan\mu_C} \left[ \frac{2(V'_C - V_A)}{V_C + V_A} - \frac{\frac{\tan\mu_A \sin\mu_A \sin\theta_A}{r_A \cos(\theta_A + \mu_A)} + \frac{\tan\mu_C \sin\mu_C \sin\theta_C}{r_C \cos(\theta_C + \mu_C)}}{2} (x_C - x_A) \right] \quad (3.37)$$

9. C' and its flow properties are now the starting point for the remaining web.

## 4 Axisymmetric Method of Characteristics Implementation

Section 3.3.1 highlights the iterative process used to determine the flow properties of a point between two fully defined points within a web of characteristic lines. However, when applying the axisymmetric MOC, this procedure is merely used as a tool. This section will explain the assumptions, inputs and process developed to execute the axisymmetric MOC used to design a nozzle's contour.

### 4.1 Assumptions

The following assumptions must be made correctly to use the axisymmetric MOC. These assumptions are necessary due to the iterative nature of the procedure.

#### 4.1.1 Initial Nozzle Length

The initial nozzle length can be described as the length along the nozzle's axis in which the expansion occurs. For illustrative purposes, this length can be seen in figure 3.1.1 as the distance from point b to point 34. When using the axisymmetric MOC for the design of a nozzle, this length must initially be assumed. This value may be iterated over if the expansion ratio calculated does not converge with the quasi-1D value.

#### 4.1.2 Axis-Pressure Distribution

Like the initial nozzle length, a pressure distribution also must be assumed for the design of a nozzle's contour via axisymmetric MOC [19]. Young reports that the following pressure distributions have been used with success. These include a cosine, parabolic, and cubic pressure distributions. It should be noted that the pressure distribution selection is dependent on the desired nozzle design Mach number. Young notes that the cosine distribution is hardly useful after the nozzle throat and that parabolic pressure distribution has proven to yield reasonable results for low Mach numbers. For higher Mach numbers, the cubic distribution can be used by decreasing the value of  $q$ . The relations are listed below as equations 4.1 through 4.3.

$$\text{Cosine: } \ln(p) = \frac{1}{2} (\ln(p_t) - \ln(p_e)) \cos\left(\frac{\pi x}{l}\right) + \frac{1}{2} (\ln(p_t) + \ln(p_e)) \quad (4.1)$$

$$\text{Parabolic: } \ln(p) = l^{-2}(x - l)^2(\ln(p_t) - \ln(p_e)) + \ln(p_e) \quad (4.2)$$

$$\text{Cubic: } \ln(p) = \left[ \frac{q}{l^3} (\ln(p_t) - \ln(p_e)) \right] x^3 - \left[ \frac{2ql+3}{l^2} (\ln(p_t) - \ln(p_e)) \right] x^2 - qx + \ln(p_t) \quad (4.3)$$

Where (x) varies from the nozzle's throat through initial expansion length (l). The nozzle's exit and throat pressure are noted as  $p_e$  and  $p_t$ , respectively. Finally, the coefficient q can be used as an additional factor that allows the cubic distribution to be manipulated further. Young provides a plot that illustrates these pressure distributions.

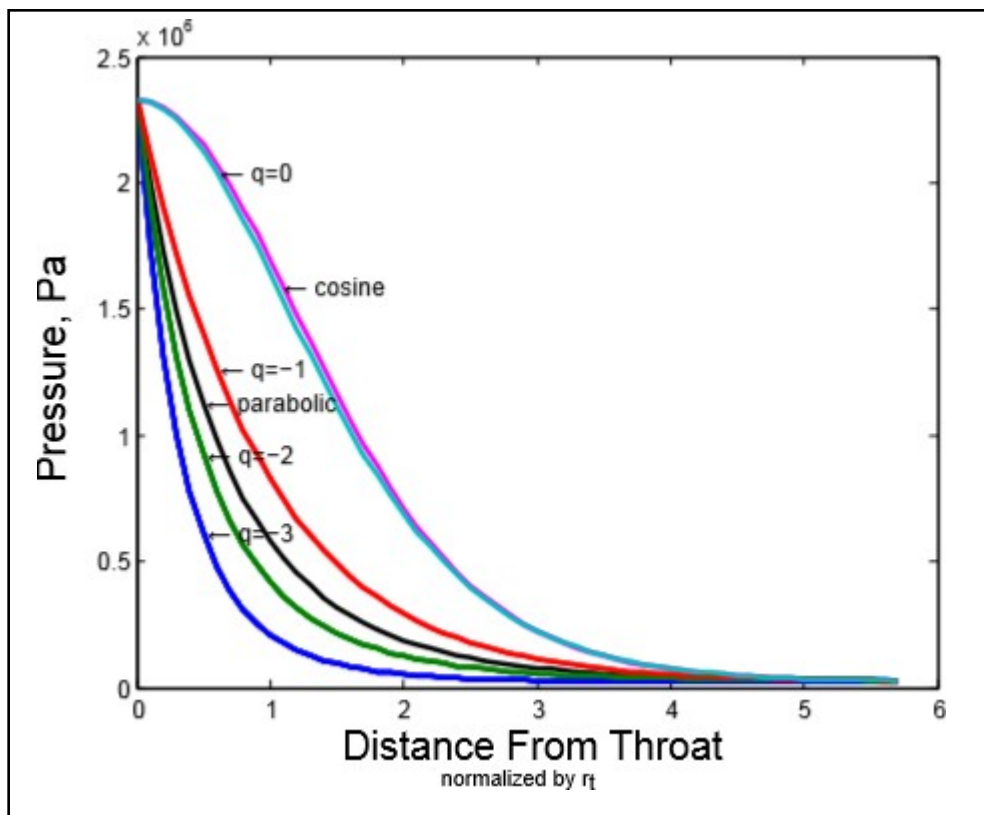


Figure 4.1.1 – Young's Pressure Distribution Plots [19]

By assuming the pressure distribution along the nozzle's centerline, each point's inclination ( $\theta$ ), Prandtl-Meyer Angle ( $\nu$ ), Mach number (M), Mach angle ( $\mu$ ), and location (x,r) are known.

## 4.2 Inputs

After the above assumptions are made, input values must be selected. The input values include design Mach number, throat location, and number of characteristic lines. It must be noted that maximizing the amount of characteristic lines used in this method will yield drastically better results. However, for computational purposes, the user is heavily limited and must select a reasonable amount. The amount of characteristic lines also determines the distance from the nozzle's throat to the intersection of the first characteristic line and the nozzle's centerline axis.

## 4.3 Implementation

Based on the assumptions, and inputs the axisymmetric MOC may now be applied to design the nozzle's contour. Figure 3.1.1 will be used as an example for the procedure. For this example, seven characteristic lines are used and the throat radius is the distance between points a and b. Additionally, the points along the nozzle centerline (points 1, 9, 16, 22, 27, 31, and 34) are fully defined due to the assumed pressure distribution. The next step is to determine the location and flow properties of points 2, 10, 17, 23, 28 and 32. This is done by following the process described in section 3.3.1. The same process can be done to calculate each "row" that occurs below the previously calculated row. Refer to figure 4.3.1 for a diagram showing the points used to calculate the next row of points.

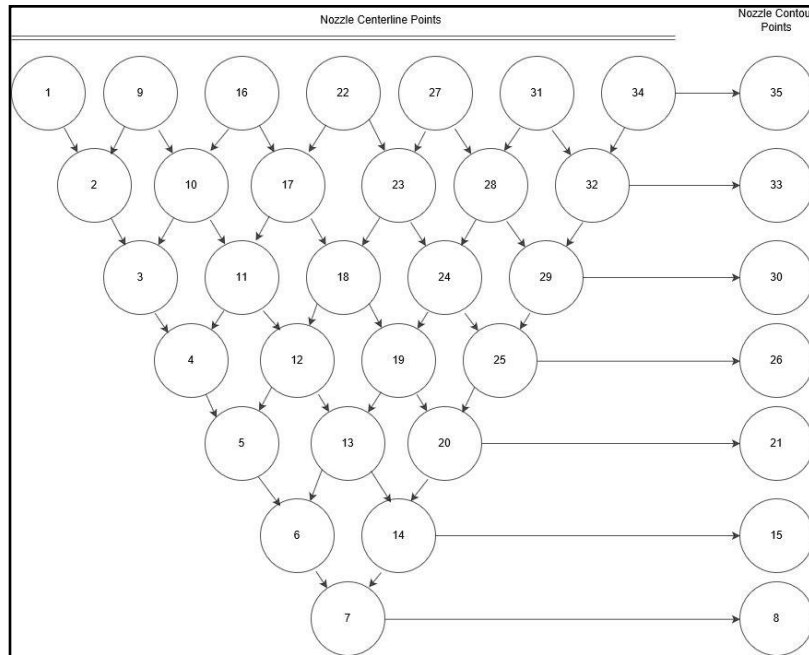


**Figure 4.3.1 – MOC Point Tree Diagram**

Once the entire point tree is defined, the nozzle contour points (wall points: 8, 15, 21, 26, 30, 33 and 35) are also known. Each of these points have the same flow properties as the previous one.

However, it must be noted that the inclination for these points is the average of the previous wall point and the point that occurs before it. For example, the inclination for point 15 will be an average of the inclinations for points 8 and 14.

After each point's location and flow properties are calculated, the area ratio can be found by comparing the radius of last point to the throat radius. This value is then checked against the area ratio that corresponds to the nozzle's design Mach number found by quasi-1D relations. If the area ratios do not match, iteration of the inputs and assumptions is required until the solution converges. This extra iteration requirement further distances this 3D MOC from the 2D MOC. Executing this process by hand can be tedious, thus a Matlab code was written to simplify this process. A colleague of mine, Irvin Quintero has contributed to this code by aiding in cumbersome indexing problems that were encountered.

#### 4.4 Converging Section Design

Although the converging section deals with subsonic flow, the design should not be overlooked. A nozzle designed with quasi 1D flow theory yields a sharp throat as seen in figure 2.1.2. However, when dealing with 2D flows, a radius of curvature is required to allow the flow to become uniform at the throat. The method used for the design of the converging section contour is Rao's method. This method uses circular arcs and the design throat radius to size the contour. Equations 4.4 and 4.5 yield the coordinates for points along the converging section. Rao developed these relationships through experimental data. Rao's method was commonly used in the 1950's for rocket nozzle design.

$$x = 1.5R_t * \cos \theta \quad (4.4)$$

$$r = 1.5R_t * \sin \theta + 2.5R_t \quad (4.5)$$

Where  $R_t$  is the throat radius and  $-130 \leq \theta \leq -90$  degrees.

#### 4.5 Axisymmetric MOC Contour

Figure 4.5.1 is the contour produced by the axisymmetric MOC method outlined in this chapter. This is a Mach 3 contour that utilizes a parabolic pressure distribution along initial nozzle length equal to the throat radius. The contour is produced using 200 characteristic lines.

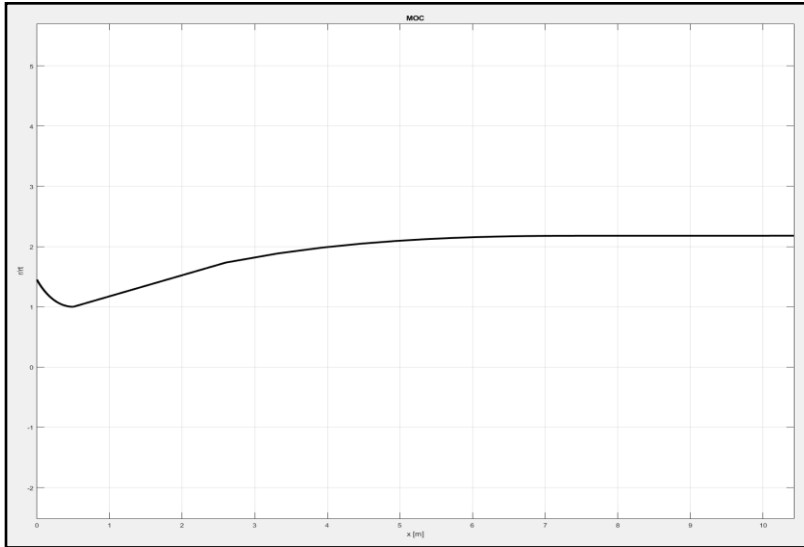


**Figure 4.5.1 – Axisymmetric MOC Designed Mach 3 Nozzle Contour**

## 5 Method Validation

Although CFD simulations are the ideal proof of validation for the method developed, due to deadline restrictions and lack of CFD software knowledge, this report does not contain CFD proof. However, Baloni designed and produced CFD simulations on a Mach 3 nozzle [21]. The CFD analysis on Baloni's nozzle is shown below in figure 5.1.1.

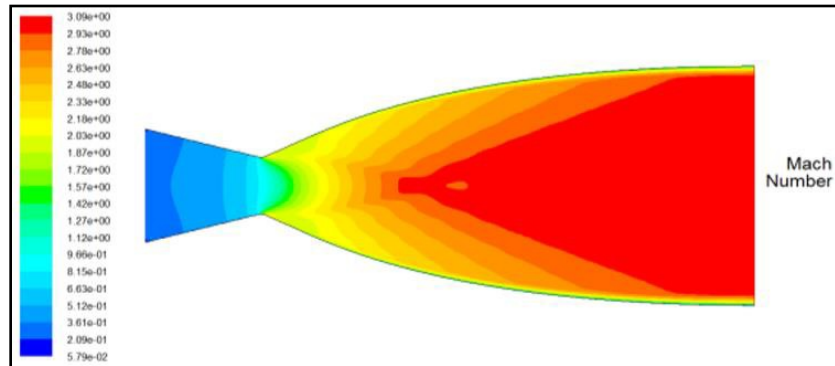


**Figure 5.1.1 – Baloni's Mach 3 Nozzle CFD Simulation**

The nozzle's geometry that Baloni designed was extrapolated via grabit.m., a free, third-party, Matlab function that allows for the extraction of points of an image. Baloni's expansion section contour was then scaled and plotted against the nozzle contour produced by the axisymmetric MOC. The axisymmetric MOC is also a Mach 3 nozzle that utilizes an initial length equal to the throat radius, parabolic pressure distribution, and 750 characteristic lines. This is shown in figure 5.1.2 below.

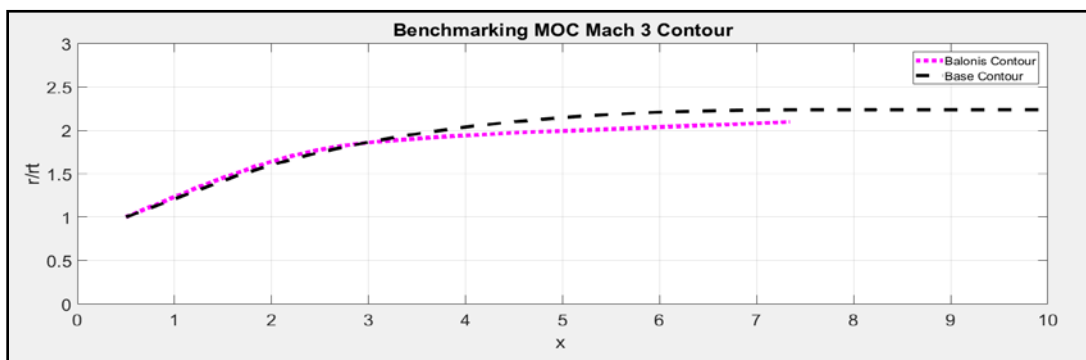


**Figure 5.1.2 – Comparison of Nozzle Contours: Baloni's Vs. Axisymmetric MOC**

The similarities of the normalized nozzle contours between Baloni and the developed axisymmetric MOC and the CFD analysis done on Baloni's contour justifies the MOC method developed.

## 6 Contour's Shape Sensitivity Analysis

As mentioned previously in the report, the methods validity is highly contingent on the assumptions made and the inputs at the start of the design process. Therefore, this section will include a sensitivity analysis of the nozzles geometry by changing alternatively, the initial nozzle length and number of characteristic lines used. The changes in the nozzle contour will then be compared against Baloni's contour. The base parameters for the one at a time analysis are a parabolic pressure distribution, initial nozzle length equal to the throat radius, and 750 characteristic lines. The nozzle produced with the base parameters is posed below in figures 6.1 and 6.2.

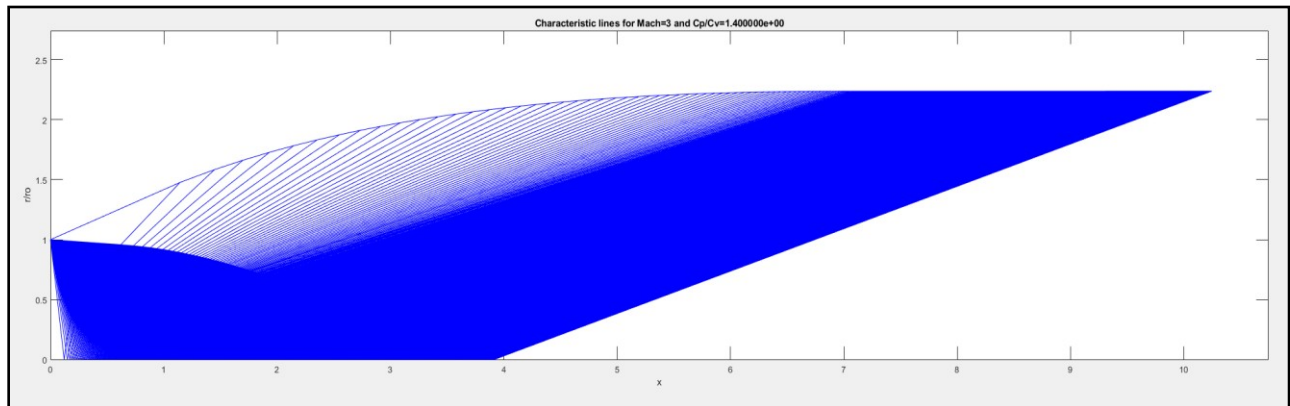


Figure 6.1 – Contour Design with Base Parameters

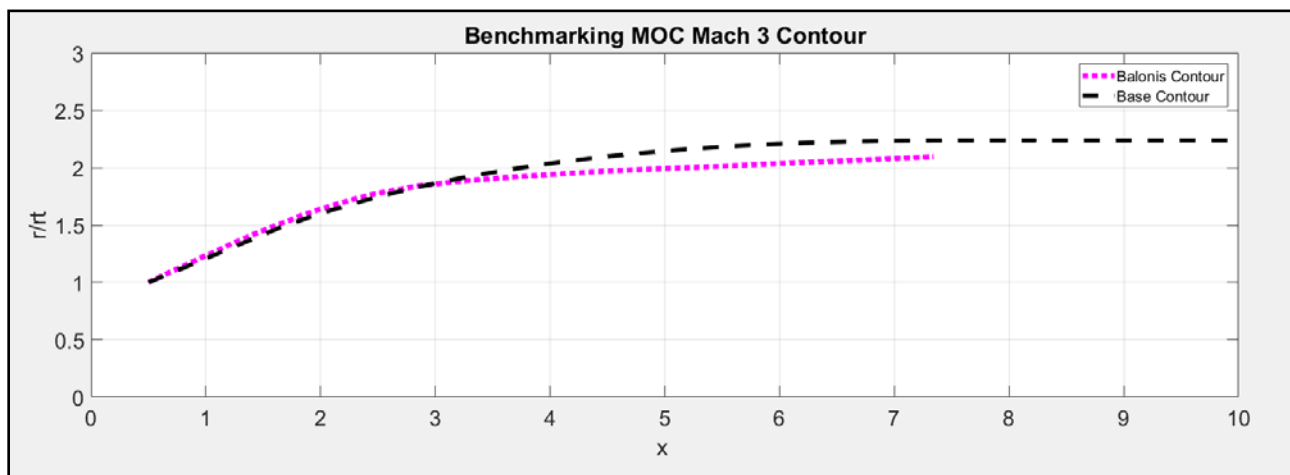
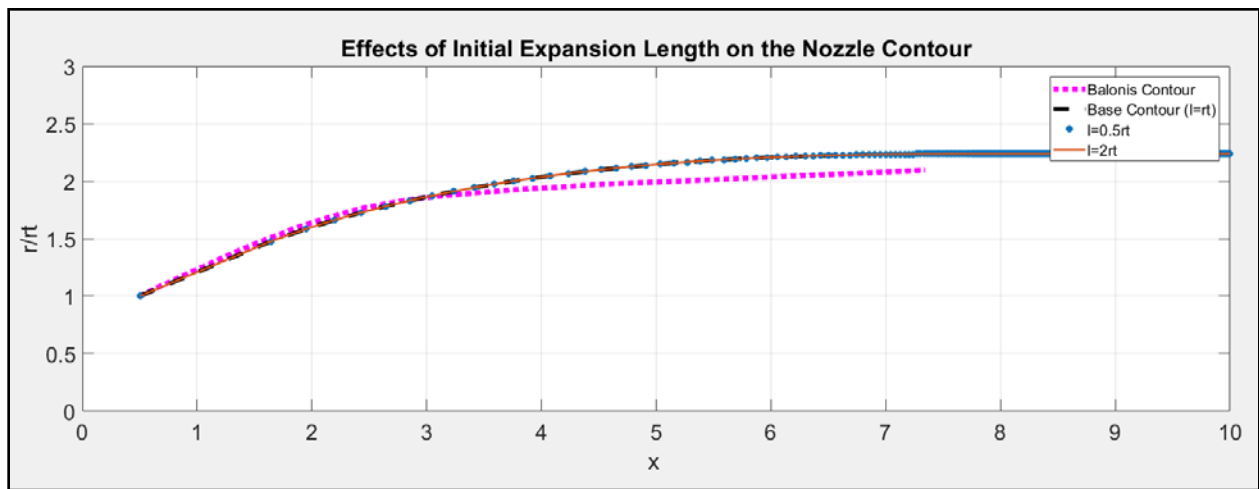


Figure 6.2 – Contour Comparison: Base Parameters Vs. Baloni's Contour

## 6.1 Effects of the Initial Nozzle Length

To examine the effects that the initial nozzle length has on the nozzle contour, three initial nozzle lengths are tested. These lengths are scaled with respect to the nozzle's throat radius. These values are as follows:  $\frac{1}{2}r_t$ ,  $r_t$  &  $2r_t$ . It should be noted that the base value for the initial nozzle length is set to  $r_t$ . Each of the contours that corresponds to the initial nozzle lengths are plotted against each other in figure 6.1.1.



**Figure 6.1.1 – Analyzing the Effects of Initial Nozzle Length on Contour**

Figure 6.1.1 validates the axisymmetric MOC contour for initial nozzle lengths between half of the throat radius and double the throat radius. This statement holds true for a parabolic pressure distribution and 750 characteristic lines. To quantify the differences between the contours produced by each variation of the initial nozzle length, Baloni's contour was used to calculate the percent error for each contour. Once the flow through the nozzle has straightened (when change in inclination is constant) the contour designed via MOC is shortened to the length of Baloni's contour for this comparison. The percent error is plotted against the horizontal distance along the nozzle contour in figure 6.1.2.

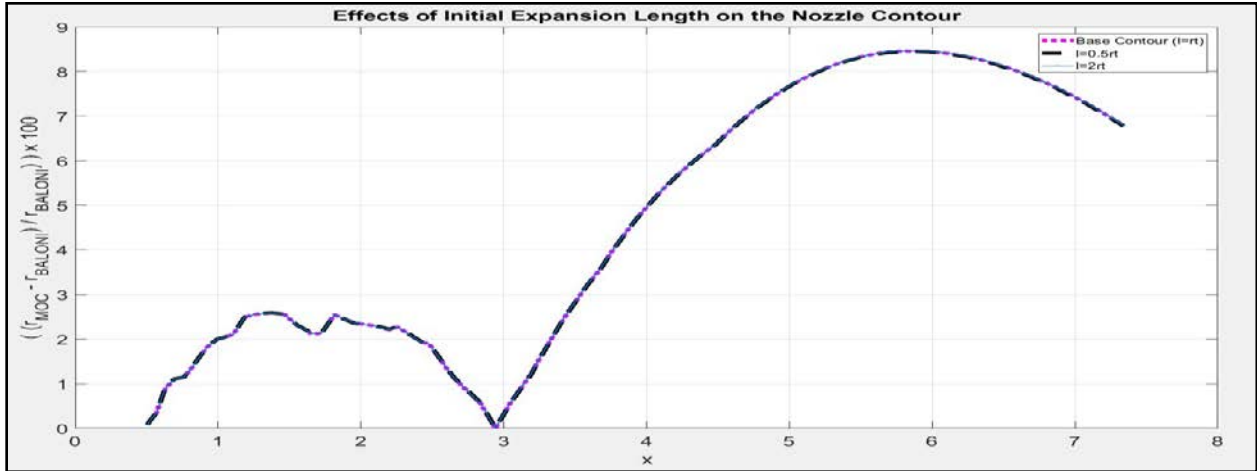


**Figure 6.1.2 – Percent Error for Varying Initial Nozzle Length**

Based off the curves, for this range of initial nozzle lengths, the overall contour of the nozzle design does not vary. The maximum error occurs near the throat of the nozzle. The error at this point is 8.4%.

## 6.2 Effects of the Number of Characteristic Lines

To examine the effects that the number of characteristic lines have on the nozzle contour, four values are tested. These values are as follows: 135, 250, 750 and 1000. It should be noted that 750 characteristic lines is used as the base value. Each of the contours that corresponds to the number of characteristics are plotted against each other in figure 6.2.1.

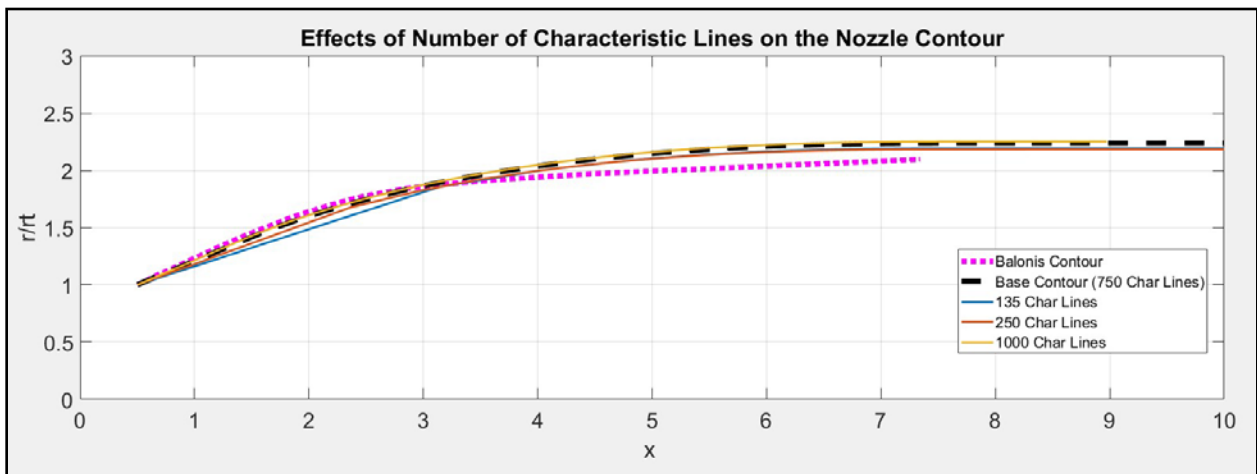


**Figure 6.2.1 – Analyzing the Effects of Amount of Characteristic Lines on Contour**

Figure 6.2.1 shows that increasing the number of characteristic lines will yield more accurate results on the initial expansion of the nozzle's contour. This statement holds true for a parabolic pressure distribution and initial expansion length equal to the radius of the throat. To quantify the differences between the contours produced by varying the number of characteristic lines, Baloni's contour was used to calculate the percent error for each contour. The percent error is plotted against the horizontal distance along the nozzle contour in figure 6.2.2.

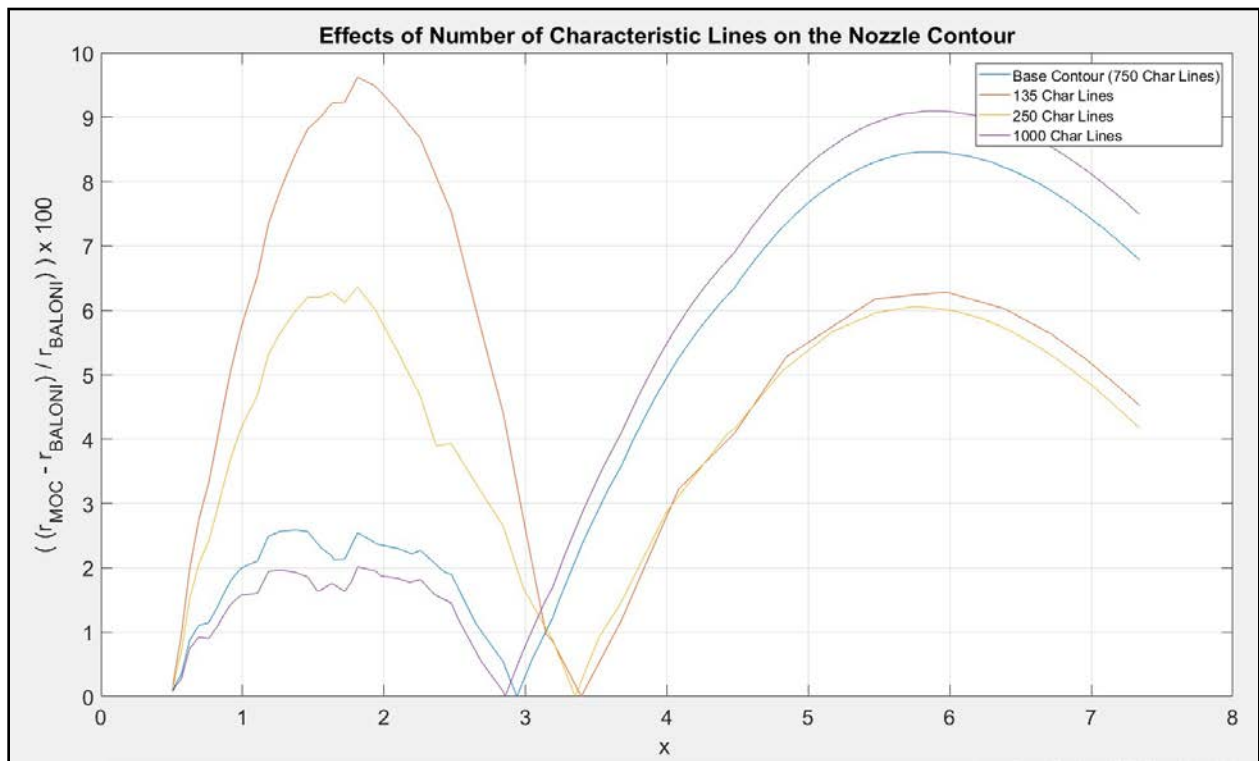


**Figure 6.1.2 – Percent Error for Varying Number of Characteristic Lines**

Figure 6.1.2 shows that increasing the number of characteristic lines minimizes the error near the initial expansion (near the throat) of the contour. A higher resolution near the initial expansion allows for more gradual expansion which ensures that oblique shocks do not form. It should also be noted that increasing the number of characteristic lines yield a greater error near the exit of the nozzle. Nonetheless, compared to the exit of the nozzle, the importance of the initial expansion

producing a shock free flow is more critical for a successful design. Additionally, the error that occurs near the exit of the nozzle is less than the error produced near the initial expansion. The maximum error occurs near the throat of the nozzle for the 135 characteristic line nozzle.

### 6.3 Results

This report produced a design method for an axisymmetric supersonic nozzle. Furthermore, quasi-1D flow and the 2D MOC was also covered. Finally, the designed nozzle contour was compared against historical data and a sensitivity analysis was done. Figures 7.1 and 7.2 below illustrate the Mach 3 nozzle contour designed by the axisymmetric MOC. This contour was designed with a parabolic pressure distribution, initial nozzle length equal to the throat radius, and 1000 characteristic lines.

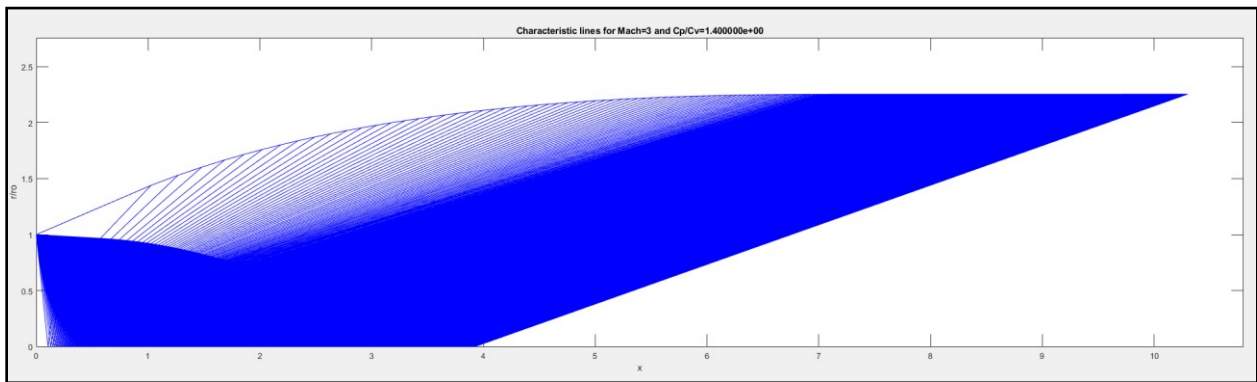


Figure 6.3.1 – Axisymmetric MOC Mach 3 Nozzle

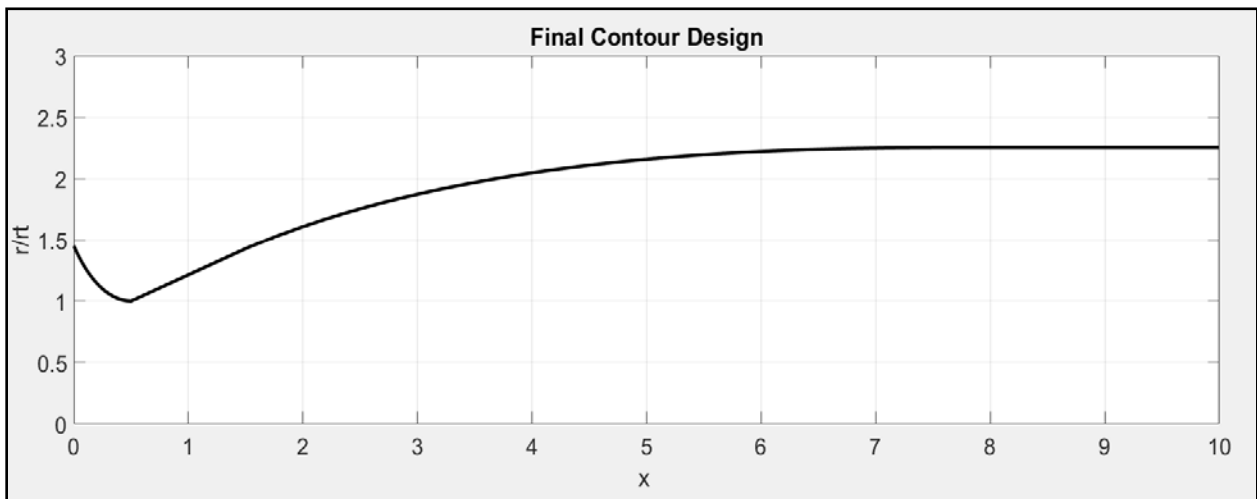


Figure 6.3.2 – Mach 3 Nozzle Contour with Rao Convergent Section

## **Future Work**

This report proved the validity of the axisymmetric MOC design method developed. Future works will include additional sensitivity analysis on the axis-pressure distribution. This will be done by changing the current pressure distribution to the cosine and cubic distribution listed in equations 4.1 and 4.3. Another sensitivity analysis will be done on the throat radius, determining a range in throat radii in which the method developed is valid.

Additionally, inviscid, laminar, and turbulent axisymmetric CFD simulations that will allow for concrete visualization of the flow throughout the nozzle. Analysis on the viscous simulations will determine if adjustments to the nozzle's contour is required to accommodate the effects of the boundary layer.

Finally, a 3D CAD model will be created with engineering drawings for the nozzle to be manufactured.

This will be submitted to conferences and journal papers in the future.

## References

- 1 “What Are Wind Tunnels?” Edited by Flint Wild, NASA, NASA, 29 Apr. 2015,  
[www.nasa.gov/audience/forstudents/k-4/stories/nasa-knows/what-are-wind-tunnels-k4.html](http://www.nasa.gov/audience/forstudents/k-4/stories/nasa-knows/what-are-wind-tunnels-k4.html).
- 2 The Space Race, History, URL: <<https://www.history.com/topics/space-race>>, retrieved Jun. 21, 2018.
- 3 SpaceX Ponders Hypersonic Decelerator for Second-stage Recovery, Aviation Week, URL:  
<<https://aviationweek.com/space/spacex-ponders-hypersonic-decelerator-second-stage-recovery>>, retrieved Jun. 21, 2018.
- 4 Six Private Companies that Could Launch Humans into Space, Space, URL:  
<<https://www.space.com/8541-6-private-companies-launch-humans-space.html>>, retrieved Jun. 21, 2018.
- 5 Wind Tunnel Design, NASA, URL: <<https://www.grc.nasa.gov/www/K12/airplane/tunpart.html>>, retrieved Jun. 21, 2018.
- 6 Wind Tunnel Parts, NASA, URL: <<https://www.grc.nasa.gov/WWW/k-12/airplane/tunnoz.html>>, retrieved Jun. 21, 2018.
- 7 Anderson, J. D. Jr., “Quasi-One-Dimensional Flow,” *Modern Compressible Flow*, 2nd ed., McGraw-Hill, New York, 1990, pp. 147-184
- 8 Anderson, J. D. Jr., “Compressible Flow through Nozzles, Diffusers, and Wind Tunnels,”  
*Fundamentals of Aerodynamics*, 5th ed., McGraw-Hill, New York, 2011, pp. 681-696
- 9 Butler, K, Cancel, D, Earley, B, Morin, S, Worcester Polytechnic Institute, *Design and Construction of a Supersonic Wind Tunnel*, 16 March 2010.
- 10 Anderson, J. D. Jr., “Oblique shock and Expansion Waves,” *Modern Compressible Flow*, 2nd ed., McGraw-Hill, New York, 1990, pp. 100-140
- 11 Anderson, J. D. Jr., “Numerical Techniques for Steady Supersonic Flow,” *Modern Compressible Flow*, 2nd ed., McGraw-Hill, New York, 1990, pp. 260-306
- 12 Hartfield, R. J., Burkhalter, J. E., A Complete and Robust Approach to Axisymmetric Method of Characteristics for Nozzle Design., *51<sup>st</sup> AIAA/SAE/ASEE Joint Propulsion Conference 2015.*, Orlando, Florida, USA, 27-29 July 2015.

- 13 Rakich, John V., "A Method of Characteristics for Steady Three-Dimensional Supersonic Flow with Application to Inclined Bodies of Revolution." NASA TN D-5341, 1969.
- 14 Zucrow, M.J., Hoffman, J.D., "Introduction to the Method of Characteristics with Application to Steady Two-Dimensional Irrotational Supersonic Flow," *Gas Dynamics*, vol. 1, John Wiley & Sons Inc, 1975, pp. 580-621
- 15 McCabe, A. Design of a Supersonic Nozzle, *University of Manchester – Aeronautical Research Council Reports and Memoranda*, 1967.
- 16 Crown, J.C., Heybey, W. H., Supersonic Nozzle Design, *Naval Ordnance Laboratory Memorandum 10594*, April 1950.
- 17 Anderson, J. D. Jr., "Inviscid, Incompressible Flow, Figure 3.5" *Fundamentals of Aerodynamics*, 5th ed., McGraw-Hill, New York, 2011, pp. 212.
- 18 Deng, Yousheng, "Design of a Two-Dimensional Supersonic Nozzle for Use in Wind Tunnels," San Jose State University, 2018.
- 19 Young, R.B, "Automated Nozzle Design through Axis-Symmetric Method of Characteristics Coupled with Chemical Kinetics," Auburn University Thesis, 2012.
- 20 "Liquid Rocket Engine Nozzles", NASA SP-8120, July 1976.
- 21 "Exhaust Nozzle Contour for Optimum Thrust," G.V.R. Rao, *Jet Propulsion* 28, pp 377, 1958.
- 22 Baloni, B. D., Kumar, S. P., Channiwalla, S. A., "Computational Analysis of Bell Nozzles," SVNIT, Surat, India. August 2017.

## **Appendices**

Appendix A: Intersect C Matlab Code

Appendix B: AxisMOC Matlab Code

Appendix C: Benchmarking Matlab Code

Appendix D: Nozzle Contour Coordinates

## Appendix A: Intersect C Matlab Function

```
function [ M_ ,Mu_ , Nu_ , xx_ , r_ , theta_ ] = intersectC( Mach, xx )
%Calc points between char lines.

%% Set up
g = 1.4; %specific heat ratio
% del = (g-1)/2; %del of air
% A_star = 2; %[in^2] %nozzle throat area
% x_star = 0; %[in] %horizontal distance from throat
% r_star = sqrt(A_star/pi); %[in] %radial distance from nozzle centerline
@throat
a = 343; %[m/s] %speed of sound
% M = 1; %Mach number at throat

%% Assume Point A & B properties
% Point A properties
M_A = Mach(1); %Mach number at point A
mu_A = asind(1/M_A); %[deg] %Mach angle at point A
% theta_A = input('Theta at Point A: '); %theta at point A
theta_A = .00002; %[deg] %inclination
x_A = xx(1); %[in] %horizontal distance from throat
r_A = 0.001; %[in] %radial distance from nozzle centerline
V_A = M_A*a; %[m/s] %velocity at point A
geom1_A = (tand(mu_A)*sind(mu_A)*sind(theta_A))/(r_A*cosd(theta_A+mu_A));
%Geometry 1 Bunch of Point A

% Point B properties
M_B = Mach(2); %Mach number at point B
mu_B = asind(1/M_B); %[deg] %Mach angle at point B
theta_B = .00002; %[deg] %inclination
x_B = xx(2); %[in] %horizontal distance from throat
r_B = 0.001; %[in] %radial distance from nozzle centerline
V_B = M_B*a; %[m/s] %velocity at point B
geom2_B = (tand(mu_B)*sind(mu_B)*sind(theta_B))/(r_B*cosd(theta_B-mu_B));
%Geometry 2 Bunch of Point B

%% Calculate Point C Location & Properties
xx_ = (r_A-r_B+(x_B*tand(theta_B-mu_B))-
(x_A*tand(theta_A+mu_A)))/(tand(theta_B-mu_B)-tand(theta_A+mu_A)); %[in]
%horizontal distance from throat
r_ = r_A + ((xx_-x_A)*tand(theta_A+mu_A)); %[in] %radial distance from nozzle
centerline
V_C = ((cotd(mu_A)*(1+(geom1_A*(xx_-x_A))))+(cotd(mu_B)*(1+(geom2_B*(xx_-
x_B)))) + theta_B - theta_A)/((cotd(mu_A)/V_A)+(cotd(mu_B)/V_B)); %[m/s]
%velocity at point C
theta_ = theta_A + cotd(mu_A)*(((V_C-V_A)/V_A)-(geom1_A*(xx_-x_A))); %[deg]
%inclination at point C
M_C = V_C/a; %Mach number at point C
mu_C = asind(1/M_C); %Mach angle at point C
geom1_C = (tand(mu_C)*sind(mu_C)*sind(theta_))/(r_*cosd(theta_+mu_C));
%Geometry 1 Bunch of Point C
geom2_C = (tand(mu_C)*sind(mu_C)*sind(theta_))/(r_*cosd(theta_-mu_C));
%Geometry 2 Bunch of Point C
```

```

%% First Iteration: Properties of A', B', and C'
% Point C' Properties
% x_C1 = (r_A-r_B+(0.5*x_B*(tand(theta_B-mu_B)+tand(theta_-mu_C)))-
(0.5*x_A*(tand(theta_A-mu_A)+tand(theta_+mu_C)))/(0.5*(tand(theta_B-
mu_B)+tand(theta_-mu_C)-tand(theta_A+mu_A)-tand(theta_+mu_C))); %[in]
%horizontal distance from throat
% r_C1 = r_A+(((xx_-x_A)/2)*(tand(theta_A+mu_A)+tand(theta_+mu_C))); %[in]
%radial distance from nozzle centerline
V_C1 = (
((2/(tand(mu_A)+tand(mu_C)))*((2*V_A)/(V_A+V_C))+(((geom1_A+geom1_C)/2)*(xx_
-
x_A)))+((2/(tand(mu_B)+tand(mu_C)))*((2*V_B)/(V_B+V_C))+(((geom2_B+geom2_C)
/2)*(xx_-x_B))))+theta_B-theta_A ) / (
4*((inv(V_A+V_C)*inv(tand(mu_A)+tand(mu_C)))+(inv(V_B+V_C)*inv(tand(mu_B)+tan
d(mu_C)))) ); %[m/s] %velocity at point C'
% theta_C1 = theta_A+((2/(tand(mu_A)+tand(mu_C)))*((2*(V_C1-V_A)/(V_C+V_A))-
(((geom1_A+geom1_C)/2)*(xx_-x_A)))); %[deg] %inclination at point C'
M_ = V_C1/a; %Mach number at point C'
Mu_ = asind(1/M_); %Mach angle at point C'
Nu_ = (sqrt((g+1)/(g-1))*atand(sqrt(((g-1)/(g+1))*((M_^2)-1)))-
atand(sqrt((M_^2)-1)));

end

```

## Appendix B: AxisMOC Matlab Code

```
% Axis-symmetric MOC Solver
clear; clc; clf; close all;

%% Set up
% Me = input('Select Desired Mach Number: ');
Me=3;
% rt = input('Select Nozzle Throat Radius [in]: ');
rt = 0.4722; %[in] %Throat radius
% l = input('Select Nozzle Length [in]: ');
l=rt;
% n_CL = input('Select Number of Characteristic Lines: ');
n_CL = 200;
syms k
n = double(symsum(k+1,k,0,n_CL))-1; %Number of characteristic points
corresponding to #char lines.
mu_e = asind(1/Me); %[deg] %Mach angle at exit
Mt = 1.001; %Mach number at throat
mu_t = asind(1/Mt); %[deg] %Mach angle at throat
theta_t = 24.88; %[deg] %Expansion angle at throat (theta max)
g = 1.4; %specific heat ratio
Pe = 101325/2; %[Pa] %Exit pressure
Pe_Po = 0.0272257; %Pe/Po for a Mach 3, isentropic expansion
Pt_Po = 0.528; %P*/Po for choked supersonic flow at throat
theta_centerline = 2E-6; %[deg] %inclination

% Vary x from throat to expansion length
X = linspace(0,1,1E6); %[in] %varying x from throat(x=0) to nozzle exit(x=1)
X_rt = X./rt; %varying x normalized by throat radius

% Solving for Pressure at throat
Pt = Pt_Po*(1/Pe_Po)*Pe; %[Pa] %Pressure at throat

%% Centerline Pressure Distribution
% Parabolic (Young Chapter 2, eq 2.4)
% Find Pressure distribution
ln_P_paral = (1.^(-2)).*((X-1).^2).*(log(Pt)-log(Pe)) + log(Pe);
P_paral = exp(ln_P_paral); %Pressure along nozzle centerline varying with x

% Plot
figure(1)
plot(X,P_paral)
hold on
grid on
xlabel('Distance from Throat [in]')
ylabel('Pressure [Pa]')
title('Pressure Distribution Along Expansion Length Centerline')

%% Extrapolate Mach number at each point along centerline
% Calc Pressure at each dx step along nozzle centerline
dx = l/n_CL; %[in] %change in x along nozzle centerline
n_char = linspace(1,n_CL,n_CL); %number of characteristics
x = n_char.*dx; %[in] %distance along nozzle centerline
ln_P_parax = (1.^(-2)).*((x-1).^2).*(log(Pt)-log(Pe)) + log(Pe);
```

```

P_x = exp(ln_P_parax); %Pressure along nozzle centerline varying with x
Po = (1/Pe_Po)*Pe; %[Pa] %Total pressure (Conserved through isentropic flow
throughout nozzle)

% Index points along nozzle wall and centerline
wallPntIndex(1) = n_CL+1;
centerPntIndex(1) = 1;
j = n_CL;
for i = 1:n_CL-1
    wallPntIndex(i+1) = wallPntIndex(i)+j;
    centerPntIndex(i+1) = wallPntIndex(i)+1;
    j = j-1;
end
WPI = [0 wallPntIndex];

% Calc Mach number at each point
Po_P_x = Po./P_x; %Po/P for each point along nozzle centerline
M = ((Po_P_x.^((g-1)/g)-1)./((g-1)/2)).^0.5;
MU = asind(1./M); %[deg] %Mach angle at point
NU = (sqrt((g+1)./(g-1)).*atand(sqrt((g-1)./(g+1)).*((M.^2)-1)))-
atand(sqrt((M.^2)-1)));

%% Calculate points b/w centerline points
i = 1;
while i < n_CL
    MACH = [M(i) M(i+1)];
    XCOMP = [x(i) x(i+1)];
    [ M_(i) ,Mu_(i), Nu_(i), xx_(i), r_(i), theta_(i)] = intersectC( MACH,
XCOMP );
    i = i+1;
end
NuNew_ = [Nu_ Nu_(end)];
thetaNew_ = [theta_ theta_(end)];

%% Calculate K+ values
j = 1;
i=1;
val = 0;
kplus = zeros(1,n_CL);
for a = 1:n_CL
    for i = 1: (n_CL+1) - val
        if a == n_CL
            kplus(end+1) = (0);
        else
            kplus(i+WPI(a)) = (thetaNew_(a)-theta_centerline) - (NuNew_(a) -
NU(a));
        end
    end
    j = j+1;
    val = val+1;
end
% kplus = [kplus];
kplus(end) = 0;
%% Calculate K- values
for i = 1:n_CL - 1
    km(i+1) = (theta_centerline - thetaNew_(i))+ ( NU(i+1) - NuNew_(i));

```

```

end
for k = 1:n_CL
    for i = 1:length(km)
        kminus(i+centerPntIndex(k)) = km(i);
    end
    km(1) = [];
end
kminus(1) = [];

for i = 2:length(kminus)
    if kminus(i)==0
        kminus(i) = kminus(i-1);
    end
end
kminus(end+1) = kminus(end);

%% Solving for thetas and nus
% indexing thetas and nus
j=1;
k=1;
THETA = zeros(1,n-1);
nu = zeros(1,n-1);
for i = 1:n-1
    if i == centerPntIndex(j)
        THETA(i) = theta_centerline;
        nu(i) = NU(j);
        nu(i+1) = NuNew_(j);
        THETA(i+1) = thetaNew_(j);
        j=j+1;
    end
end

% Solving for thetas and nus
nn = 6;
for k = 1:n_CL-2
    p = 1;
    for i = 1 : length(THETA)-nn
        if THETA(i) == thetaNew_(p)
            if i == (length(THETA)- 3)
                THETA(i) = abs(THETA(i));
            else
                THETA(i+1) = abs((thetaNew_(p+1)+NuNew_(p+1)+thetaNew_(p)+
kplus(i+1) - kminus(i+1) - NuNew_(p))/2);
                nu(i+1) = THETA(i+1) - thetaNew_(p) - kplus(i+1) + NuNew_(p);
                thetaNew_(p) = abs(THETA(i+1));
                NuNew_(p) = nu(i+1);
            %
            THETA(i+1) = (THETA(i+1)+nu(i+1)+THETA(i)+ kplus(i+1) -
kminus(i+1) - nu(i))/2;
            %
            nu(i+1+k) = THETA(i+1) - thetaNew_(p) - kplus(i+1) + NuNew_(p);
        end

        if p < length(thetaNew_)
            p = p+1;
        end
    end
end
end

```

```

    nn = nn+(3)+k;
end

for a = 2:length(THETA)-1
    if THETA(a) == theta_centerline
        THETA(a-1) = abs(THETA(a-2));
        THETA(end) = abs(THETA(end-1));
        nu(a-1) = nu(a-2);
        nu(end) = nu(end-1);
    end
end

%% Solving for Mach# and MU
for b = 1:length(nu)
    [Mnum(b),NU_, mu(b)] = flowprandtlmeyer(g, nu(b), 'nu');
    SUM_thetaMU(b) = THETA(b) + mu(b); %[deg] %theta+Mu
    DIFF_thetaMU(b) = THETA(b) - mu(b); %[deg] %theta-Mu
end

d = 0;
for c = 2:length(THETA)
    if (THETA(c) == theta_centerline) && (c == n_CL+2)
        SUM_thetaMU(c-1) = (theta_t + THETA(c-1))/2; %[deg] %theta+Mu
        DIFF_thetaMU(c-1) = 0; %[deg] %theta-Mu
    elseif c == length(THETA)

        SUM_thetaMU(c) = (SUM_thetaMU(end-2) + THETA(c))/2; %[deg] %theta+Mu
        DIFF_thetaMU(c) = 0; %[deg] %theta-Mu
    elseif (THETA(c) == THETA(c-1)) && (c > n_CL+2)
        SUM_thetaMU(c) = ((SUM_thetaMU(c-(n_CL-d)) + THETA(c))/2); %[deg]
%theta+Mu
        DIFF_thetaMU(c) = 0; %[deg] %theta-Mu
        d = d+1;
    end
end

%% Table
Point = [1:n]';
K_minus = kminus';
K_plus = kplus';
Theta = THETA';
Nu = nu';
Mach = Mnum';
Mu = mu';
Sum = SUM_thetaMU';
Diff = DIFF_thetaMU';

T = table(Point,K_minus,K_plus,Theta,Nu, Mach, Mu, Sum, Diff);

% filename = 'testdata.xlsx';
%writetable(T,filename)

%% Grid generator
figure(2)
D=1; % Non-Dimensional y co-ordinate of throat wall
i=1;

```

```

x=zeros(1,n);
r=zeros(1,n);
wall=theta_t;
while (i<=n_CL+1)
    if i==1
        x(i)=-D/(tand(THETA(i)-mu(i)));
        r(i)=0;
        plot([0 x(i)],[D 0], 'b');
        hold on
    else if i==n_CL+1
        x(i)=(r(i-1)-D-x(i-1)*tand((THETA(i-1)+THETA(i)+mu(i-1)+mu(i))*0.5))/(tand(0.5*(wall+THETA(i)))-tand((THETA(i-1)+THETA(i)+mu(i-1)+mu(i))*0.5));
        r(i)=D+x(i)*tand(0.5*(wall+THETA(i)));
        plot([x(i-1) x(i)],[r(i-1) r(i)], 'b');
        hold on
        plot([0 x(i)],[D r(i)], 'b');
        hold on
    else
        x(i)=(D-r(i-1)+x(i-1)*tand(0.5*(mu(i-1)+THETA(i-1)+mu(i)+THETA(i))))/(tand(0.5*(mu(i-1)+THETA(i-1)+mu(i)+THETA(i)))-tand(THETA(i)-mu(i)));
        r(i)=tand(THETA(i)-mu(i))*x(i)+D;
        plot([x(i-1) x(i)],[r(i-1) r(i)], 'b');
        hold on
        plot([0 x(i)],[D r(i)], 'b');
        hold on
    end
end
i=i+1;
hold on
end
h=i;
k=0;
i=h;
for j=1:n_CL-1
    while (i<=h+n_CL-k-1)
        if (i==h)
            x(i)=round(x(i-n_CL+k)-r(i-n_CL+k)/(tand(0.5*(THETA(i-n_CL+k)+THETA(i)-mu(i-n_CL+k)-mu(i))))),4);
            r(i)=0;
            plot([x(i-n_CL+k) x(i)],[r(i-n_CL+k) r(i)], 'b');
            hold on
        else if (i==h+n_CL-k-1)
            x(i)=(x(i-n_CL+k)*tand(0.5*(THETA(i-n_CL+k)+THETA(i)))-r(i-n_CL+k)+r(i-1)-x(i-1)*tand((THETA(i-1)+THETA(i)+mu(i-1)+mu(i))*0.5))/(tand(0.5*(THETA(i-n_CL+k)+THETA(i)))-tand((THETA(i-1)+THETA(i)+mu(i-1)+mu(i))*0.5));
            r(i)=r(i-n_CL+k)+(x(i)-x(i-n_CL+k))*tand(0.5*(THETA(i-n_CL+k)+THETA(i)));
            xwall(i) = round(x(i),4);
            rwall(i) = round(r(i),4);
            plot([x(i-1) x(i)],[r(i-1) r(i)], 'b');
            hold on
            plot([x(i-n_CL+k) x(i)],[r(i-n_CL+k) r(i)], 'b');
            hold on
        else

```

```

s1= round(tand(0.5*(THETA(i)+THETA(i-1)+mu(i)+mu(i-1))),4);
s2= round(tand(0.5*(THETA(i)+THETA(i-n_CL+k)-mu(i)-mu(i-
n_CL+k))),4);
x(i)=round((r(i-n_CL+k)-r(i-1)+s1*x(i-1)-s2*x(i-n_CL+k))/(s1-
s2),4);
r(i)=round(r(i-1)+(x(i)-x(i-1))*s1,4);
plot([x(i-1) x(i)], [r(i-1) r(i)], 'b');
hold on
plot([x(i-n_CL+k) x(i)], [r(i-n_CL+k) r(i)], 'b');
hold on
end
end
i=i+1;
end
k=k+1;
h=i;
i=h;
hold on
end
title(sprintf('Characteristic lines for Mach=%d and Cp/Cv=%d',Me,g))
xlabel('x');
ylabel('r/ro');
axis equal
xlim([0 x(n)+0.5])
ylim([0 r(n)+0.5])

for z = 1: length(wallPntIndex)
XWALL1(z) = round(x(wallPntIndex(z)),4);
RWALL1(z) = round(r(wallPntIndex(z)),4);
MWALL1(z) = round(Mnum(wallPntIndex(z)),4);
end
XWALL = round([0 XWALL1],4);
RWALL = round([1 RWALL1]*rt,4);
MWALL = round([1 MWALL1],4);

% figure(3)
% plot(XWALL*rt,RWALL./rt,'.-')
% hold on
% axis equal
%
xwall = XWALL';
rwall = RWALL';
% contour = table(xwall,rwall);
% hold off

% filename = 'testdata.xlsx';
% writetable(contour,filename)

%% Plotting Contour
% M = Mnum;
% xw = xwall';
% yw = rwall'./rt;
% [X, R] = meshgrid (unique(sortrows(x(:))),unique(sortrows(r(:))));
% M_interp = griddata(x,r,M,X,R);
% figure (4)

```

```

% set(gcf, 'color', [1 1 1], 'numbertitle', 'off', 'name', 'Mach Number
contour', 'colormap', jet)
% contourf(X,R,M_interp,10);
% hold on
% contourf(X,-R,M_interp,10);
% % The following two lines will allow you to plot the nozzle contour on top
of the surface plot. xwall and ywall are the coordinates of the nozzle's
contour
% plot(xw,yw,'k-','LineWidth',3)
% plot(xw,-yw,'k-','LineWidth',3)
% axis equal
% %axis([0 ceil(xw(length(xw),1)) -ceil(yw(length(yw),1))
ceil(yw(length(yw),1))])
% xlabel ('x/y_0');
% ylabel ('y/y_0');
% set(gca,'fontsize',16,'fontname','Times New Roman','fontweight','bold');
% axis equal
%
% disp(max(r))
% disp(max(rwall))

%% RAO Nozzle Designer
% Set up
t = linspace(0,1,1E3);
E = 4.235; %Expansion Ratio for a Mach 3 Expansion
bell = .8; %Bell Percent

% Angles taken from figure.
% Corresponds to 80% bell curve & Expansion Ratio
theta_n = 22; %[deg] %Initial theta
theta_e = 13; %[deg] %Final theta
% theta_n = 18; %[deg] %Initial theta
% theta_e = 8; %[deg] %Final theta

% Throat
% Converging Section
theta_c = linspace(-135,-90,1E3);
x_c = 1.5.*rt.*cosd(theta_c);
y_c = ((1.5.*rt.*sind(theta_c)) + (1.5.*rt) + rt)*1.025;

% Diverging Section
theta_d = linspace(-90,theta_n-90,1E3);
x_d = 0.382.*rt.*cosd(theta_d)*1.5;
y_d = ((0.392.*rt.*sind(theta_d)) + (0.382.*rt) + rt)*1.035;

% Bell Section
% Constants/Coefficients
Nx = 0.382*rt*cosd(theta_n - 90);
Ny = (0.382*rt*sind(theta_n - 90)) + (0.382*rt) + (rt);
Ex = bell*(((E^(0.5))-1)*rt)/tand(15));
Ey = (E^(0.5))*rt;
m1 = tand(theta_n);
m2 = tand(theta_e);
c1 = Ny - (m1*Nx);
c2 = Ey - (m2*Ex);

```

```

Qx = (c2 - c1)/(m1 - m2);
Qy = ((m1*c2) - (m2*c1))/(m1 - m2);

% Implementation
x_t = (((1-t).^2).*Nx) + (2.*(1-t).*t.*Qx) + ((t.^2).*Ex)*1.5;
r_t = (((1-t).^2).*Ny) + (2.*(1-t).*t.*Qy) + ((t.^2).*Ey)*1.025;

% Plot
figure(5)
plot(xwall,rwall./rt,'k','LineWidth',3);
grid on; hold on; axis equal;
plot(x_t./rt,r_t./rt,'m','LineWidth',3);
plot(x_c./rt,y_c./rt,'m','LineWidth',3);
plot(x_d./rt,y_d./rt,'m','LineWidth',3);
title('Rao Method VS. MOC Mach 3 Nozzle')
xlabel('x/rt')
ylabel('r/rt')
legend('3D-MOC','Rao')
figure(6)
plot(x_t,r_t,'k','LineWidth',3)
hold on; grid on; axis equal;
plot(x_c,y_c,'k','LineWidth',3)
plot(x_d,y_d,'k','LineWidth',3)
plot([x_c(1),x_t(end)], [0,0], 'k:', 'LineWidth', 3)
title('RAO')
xlabel('x [m]')
ylabel('r [m]')

X_C = x_c'-(x_c(1));
X_D = x_d'-(x_c(1));
R_C = y_c';
R_D = y_d';
X_T = x_t'-(x_c(1));
R_T = r_t';
Xfinal = xwall-(x_c(1));
Rfinal = rwall;
X_C = X_C;
R_C = R_C-((R_C(end))-(Rfinal(1)));
figure(7)
plot(X_C,R_C./rt,'k','LineWidth',3)
hold on; grid on; axis equal;
plot(Xfinal,Rfinal./rt,'k','LineWidth',3)
title('MOC')
xlabel('x [m]')
ylabel('r/rt')

```

## Appendix C: Benchmarking Matlab Code

```
clear
clc
clf
close all

% grabit('Capture.jpg')

%% Benchmarking

% Converging Section
rt = 0.4722;

% Import Points from Grabit
x_BenchMark =
[0.499418977981112;0.526424836274378;0.568380269883893;0.626732745102518;0.69
1836053529737;0.760796876790661;0.817716902560689;0.866799733742825;0.9191116
70111277;0.990152332879700;1.10704605917199;1.18445852913764;1.26811682891100
;1.37373525594577;1.46262191011125;1.55255363670769;1.63307412215199;1.723005
34063265;1.81422601523053;1.94155641840031;2.09259587627348;2.25768525496564;
2.47576370165701;2.84282628666465;3.19466051268668;3.67769742911057;4.4796851
4986694;5.72470133940710;7.34160579232297];
r_BenchMark =
[0.999877648625488;1.01254929834938;1.03175272976144;1.06179889030366;1.09184
507367581;1.12136873160275;1.14799428953939;1.17143719829241;1.19627968469784
;1.22881985146728;1.28007937834604;1.31830494317825;1.35513111587809;1.400738
92117584;1.43841493978271;1.47325820117115;1.50555194605529;1.53784572276461;
1.57717950412723;1.62023679619644;1.66757606626997;1.71800786562004;1.7731608
2419698;1.83960696847605;1.88039158149655;1.92006247555817;1.97087732938050;2
.02432189565859;2.09528914774671];

%% Calc Percent Errors
X = [0:.005:10];

% Benchmark nozzle
r_Bench = interp1(x_BenchMark,r_BenchMark,X);

% MOC Base
r_MOC_Base = interp1(x_Base,r_Base,X)./rt;
Base_ERR = abs(r_MOC_Base-r_Bench)./r_Bench;
Max_Base_ERR = max(Base_ERR)*100;

% Length 1: 0.5rt
r_l1 = interp1(x_L1,r_L1,X)./rt;
r1_ERR = abs(r_l1-r_Bench)./r_Bench;
Max_r1_ERR = max(r1_ERR)*100;

% Length 2: 2rt
r_l2 = interp1(x_L2,r_L2,X)./rt;
r2_ERR = abs(r_l2-r_Bench)./r_Bench;
Max_r2_ERR = max(r2_ERR)*100;

% 135 Char lines
```

```

r_135 = interp1(x_1,r_1,X)./rt;
r135_ERR = abs(r_135-r_Bench)./r_Bench;
Max_r135_ERR = max(r135_ERR)*100;

% 250 Char lines
r_250 = interp1(x_2,r_2,X)./rt;
r250_ERR = abs(r_250-r_Bench)./r_Bench;
Max_r250_ERR = max(r250_ERR)*100;

% 1000 Char lines
m = 520;
x_4 = x_4(1:m);
r_4 = r_4(1:m);
r_1000 = interp1(x_4,r_4,X)./rt;
r1000_ERR = abs(r_1000-r_Bench)./r_Bench;
Max_r1000_ERR = max(r1000_ERR)*100;

%% Plots
figure(1) %comparing initial nozzle lengths
plot(x_BenchMark,r_BenchMark,'m','LineWidth',5)
hold on; grid on; axis equal; xlim([0,10]); ylim([0,3]);
plot(x_Base,r_Base./rt,'k--','LineWidth',4)
plot(x_L1,r_L1./rt,'X','LineWidth',4)
plot(x_L2,r_L2./rt,'LineWidth',2)
xlabel('x ')
ylabel('r/rt')
title('Effects of Initial Expansion Length on the Nozzle Contour')
legend({'Balonis Contour', 'Base Contour (l=rt)', 'l=0.5rt', 'l=2rt'}, 'FontSize',14)
hold off

figure(2) %comparing number of char lines
plot(x_BenchMark,r_BenchMark,'m','LineWidth',5)
hold on; grid on; axis equal; xlim([0,10]); ylim([0,3]);
plot(x_Base,r_Base./rt,'k--','LineWidth',5)
plot(x_1,r_1./rt,'LineWidth',2)
plot(x_2,r_2./rt,'LineWidth',2)
% plot(x_3,r_3./rt,'LineWidth',2)
plot(x_4,r_4./rt,'LineWidth',2)
% plot(x_MOC,r_MOC./rt,'LineWidth',2)
xlabel('x ')
ylabel('r/rt')
title('Effects of Number of Characteristic Lines on the Nozzle Contour')
legend({'Balonis Contour', 'Base Contour (750 Char Lines)', '135 Char Lines', '250 Char Lines', '1000 Char Lines'}, 'FontSize',14)

figure(3) %final nozzle design with converging section
plot(x_MOC,r_MOC./rt,'k','LineWidth',3)
hold on; grid on; axis equal; xlim([0,10]); ylim([0,3]);
xlabel('x ')
ylabel('r/rt')
title('Final Contour Design')

figure(4)
plot(X,Base_ERR*100,'m','LineWidth',5)
hold on; grid on;

```

```

plot(X,r1_ERR*100,'k--','LineWidth',5)
plot(X,r2_ERR*100,'.-','LineWidth',1)
xlabel('x')
ylabel('( (r_M_O_C - r_B_A_L_O_N_I) / r_B_A_L_O_N_I ) x 100')
title('Effects of Initial Expansion Length on the Nozzle Contour')
legend({'Base Contour (l=rt)', 'l=0.5rt', 'l=2rt'}, 'FontSize',14)

figure(5)
plot(X,Base_ERR*100)
hold on; grid on;
plot(X,r135_ERR*100)
plot(X,r250_ERR*100)
plot(X,r1000_ERR*100)
xlabel('x ')
ylabel('( (r_M_O_C - r_B_A_L_O_N_I) / r_B_A_L_O_N_I ) x 100')
title('Effects of Number of Characteristic Lines on the Nozzle Contour')
legend({'Base Contour (750 Char Lines)', '135 Char Lines', '250 Char Lines', '1000 Char Lines'}, 'FontSize',14)

figure(6) %final nozzle design with converging section
plot(x_MOC,r_MOC./rt,'k','LineWidth',3)
hold on; grid on; axis equal; xlim([0,10]); ylim([0,3]);
xlabel('x ')
ylabel('r/rt')
title('Final Contour Design')

figure(7) %base vs baloni
plot(x_BenchMark,r_BenchMark,'m:','LineWidth',5)
hold on; grid on; axis equal; xlim([0,10]); ylim([0,3]);
plot(x_Base,r_Base./rt,'k--','LineWidth',4)
xlabel('x ')
ylabel('r/rt')
title('Benchmarking MOC Mach 3 Contour')
legend({'Balonis Contour', 'Base Contour'}, 'FontSize',14)
hold off

```

## Appendix D: Nozzle Contour Coordinates

x	r
0	0.684842674
0.00039391	0.684439233
0.00078813	0.68403611
0.001182658	0.683633304
0.001577496	0.683230817
0.001972642	0.682828648
0.002368096	0.682426798
0.002763859	0.682025266
0.003159929	0.681624053
0.003556307	0.68122316
0.003952993	0.680822586
0.004349985	0.680422332
0.004747284	0.680022398
0.00514489	0.679622785
0.005542803	0.679223492
0.005941021	0.678824519
0.006339546	0.678425868
0.006738376	0.678027538
0.007137511	0.677629529
0.007536952	0.677231843
0.007936697	0.676834478
0.008336747	0.676437435
0.008737102	0.676040715
0.009137761	0.675644318
0.009538723	0.675248244
0.00993999	0.674852493
0.010341559	0.674457065
0.010743432	0.674061961
0.011145608	0.673667181
0.011548087	0.673272726
0.011950867	0.672878594
0.012353951	0.672484788
0.012757336	0.672091306
0.013161022	0.67169815
0.01356501	0.671305319
0.0139693	0.670912814
0.01437389	0.670520634
0.014778781	0.670128781
0.015183972	0.669737254
0.015589464	0.669346054
0.015995255	0.668955181
0.016401347	0.668564634
0.016807737	0.668174416
0.017214427	0.667784524
0.017621416	0.667394961
0.018028703	0.667005726
0.018436289	0.666616819
0.018844173	0.66622824
0.019252354	0.665839991
0.019660834	0.66545207
0.020069611	0.665064479
0.020478685	0.664677217
0.020888056	0.664290285
0.021297724	0.663903683
0.021707688	0.663517412
0.022117948	0.66313147
0.022528504	0.66274586
0.022939356	0.66236058
0.023350503	0.661975632
0.023761945	0.661591015
0.024173682	0.66120673
0.024585714	0.660822777
0.02499804	0.660439156
0.02541066	0.660055867
0.025823575	0.659672911
0.026236782	0.659290287

0.026650283	0.658907997
0.027064077	0.65852604
0.027478164	0.658144417
0.027892544	0.657763128
0.028307216	0.657382172
0.02872218	0.657001551
0.029137436	0.656621264
0.029552983	0.656241313
0.029968822	0.655861696
0.030384951	0.655482414
0.030801372	0.655103468
0.031218083	0.654724857
0.031635084	0.654346582
0.032052375	0.653968644
0.032469956	0.653591042
0.032887827	0.653213776
0.033305986	0.652836848
0.033724435	0.652460256
0.034143172	0.652084002
0.034562198	0.651708085
0.034981512	0.651332506
0.035401114	0.650957265
0.035821004	0.650582363
0.036241181	0.650207799
0.036661646	0.649833573
0.037082397	0.649459687
0.037503435	0.649086139
0.037924759	0.648712932
0.038346369	0.648340063
0.038768265	0.647967535
0.039190447	0.647595346
0.039612914	0.647223498
0.040035667	0.646851991
0.040458704	0.646480824
0.040882025	0.646109999
0.041305631	0.645739514
0.041729521	0.645369371
0.042153695	0.64499957
0.042578152	0.644630111
0.043002893	0.644260994
0.043427916	0.643892219
0.043853222	0.643523787
0.044278811	0.643155698
0.044704682	0.642787951
0.045130835	0.642420548
0.045557269	0.642053489
0.045983985	0.641686773
0.046410982	0.641320402
0.04683826	0.640954374
0.047265818	0.640588691
0.047693657	0.640223353
0.048121776	0.639858359
0.048550175	0.639493711
0.048978853	0.639129408
0.049407811	0.63876545
0.049837047	0.638401839
0.050266563	0.638038573
0.050696357	0.637675653
0.051126429	0.63731308
0.051556779	0.636950854
0.051987407	0.636588975
0.052418312	0.636227442
0.052849494	0.635866257
0.053280953	0.63550542
0.053712689	0.63514493
0.054144702	0.634784789
0.05457699	0.634424995
0.055009554	0.634065551
0.055442394	0.633706454
0.055875509	0.633347707

0.056308899	0.632989309
0.056742564	0.63263126
0.057176503	0.632273561
0.057610717	0.631916212
0.058045204	0.631559212
0.058479966	0.631202563
0.058915	0.630846264
0.059350308	0.630490316
0.059785889	0.630134719
0.060221742	0.629779473
0.060657867	0.629424579
0.061094265	0.629070035
0.061530935	0.628715844
0.061967876	0.628362005
0.062405088	0.628008518
0.062842571	0.627655383
0.063280325	0.627302601
0.06371835	0.626950172
0.064156644	0.626598096
0.064595209	0.626246373
0.065034043	0.625895004
0.065473147	0.625543988
0.065912519	0.625193327
0.066352161	0.624843019
0.066792071	0.624493066
0.067232249	0.624143468
0.067672695	0.623794224
0.068113409	0.623445336
0.068554391	0.623096802
0.06899564	0.622748625
0.069437155	0.622400802
0.069878937	0.622053336
0.070320986	0.621706226
0.070763301	0.621359472
0.071205881	0.621013075
0.071648727	0.620667034
0.072091839	0.620321351
0.072535215	0.619976025
0.072978856	0.619631056
0.073422762	0.619286444
0.073866932	0.618942191
0.074311365	0.618598295
0.074756063	0.618254758
0.075201023	0.617911579
0.075646247	0.617568759
0.076091734	0.617226298
0.076537483	0.616884196
0.076983494	0.616542453
0.077429768	0.61620107
0.077876303	0.615860046
0.078323099	0.615519383
0.078770157	0.615179079
0.079217475	0.614839136
0.079665054	0.614499553
0.080112894	0.614160332
0.080560993	0.613821471
0.081009353	0.613482971
0.081457971	0.613144833
0.081906849	0.612807057
0.082355986	0.612469642
0.082805382	0.612132589
0.083255036	0.611795899
0.083704948	0.611459571
0.084155118	0.611123605
0.084605545	0.610788003
0.08505623	0.610452764
0.085507171	0.610117888
0.08595837	0.609783375
0.086409825	0.609449226
0.086861536	0.609115441

0.087313503	0.60878202
0.087765725	0.608448964
0.088218203	0.608116272
0.088670936	0.607783944
0.089123923	0.607451982
0.089577165	0.607120385
0.090030661	0.606789153
0.090484412	0.606458286
0.090938415	0.606127786
0.091392673	0.605797651
0.091847183	0.605467882
0.092301946	0.60513848
0.092756962	0.604809445
0.093212229	0.604480776
0.093667749	0.604152474
0.09412352	0.603824539
0.094579543	0.603496972
0.095035817	0.603169773
0.095492342	0.602842941
0.095949117	0.602516477
0.096406143	0.602190381
0.096863418	0.601864654
0.097320943	0.601539295
0.097778718	0.601214305
0.098236742	0.600889684
0.098695014	0.600565432
0.099153535	0.60024155
0.099612305	0.599918037
0.100071322	0.599594894
0.100530587	0.599272121
0.1009901	0.598949718
0.10144986	0.598627686
0.101909866	0.598306024
0.102370119	0.597984733
0.102830619	0.597663813
0.103291364	0.597343264
0.103752355	0.597023087
0.104213592	0.596703281
0.104675074	0.596383847
0.1051368	0.596064785
0.105598772	0.595746095
0.106060987	0.595427777
0.106523447	0.595109832
0.10698615	0.59479226
0.107449097	0.594475061
0.107912286	0.594158234
0.108375719	0.593841782
0.108839394	0.593525703
0.109303312	0.593209997
0.109767471	0.592894666
0.110231873	0.592579708
0.110696515	0.592265125
0.111161399	0.591950917
0.111626524	0.591637083
0.112091889	0.591323624
0.112557495	0.59101054
0.11302334	0.590697832
0.113489426	0.590385499
0.11395575	0.590073541
0.114422314	0.58976196
0.114889117	0.589450754
0.115356158	0.589139925
0.115823437	0.588829473
0.116290955	0.588519397
0.11675871	0.588209698
0.117226703	0.587900375
0.117694932	0.587591431
0.118163399	0.587282863
0.118632102	0.586974673
0.119101041	0.586666861

0.119570216	0.586359427
0.120039627	0.586052371
0.120509273	0.585745693
0.120979154	0.585439394
0.12144927	0.585133474
0.121919621	0.584827933
0.122390206	0.584522771
0.122861024	0.584217988
0.123332077	0.583913584
0.123803362	0.583609561
0.124274881	0.583305917
0.124746633	0.583002653
0.125218616	0.582699769
0.125690833	0.582397266
0.12616328	0.582095144
0.12663596	0.581793402
0.127108871	0.581492041
0.127582013	0.581191062
0.128055385	0.580890464
0.128528988	0.580590247
0.129002821	0.580290412
0.129476884	0.57999096
0.129951177	0.579691889
0.130425698	0.5793932
0.130900449	0.579094894
0.131375428	0.578796971
0.131850636	0.57849943
0.132326072	0.578202273
0.132801735	0.577905499
0.133277626	0.577609108
0.133753744	0.577313101
0.134230089	0.577017477
0.134706661	0.576722238
0.135183459	0.576427382
0.135660483	0.576132911
0.136137733	0.575838824
0.136615208	0.575545122
0.137092908	0.575251805
0.137570833	0.574958873
0.138048983	0.574666327
0.138527356	0.574374165
0.139005954	0.574082389
0.139484776	0.573790999
0.13996382	0.573499995
0.140443088	0.573209377
0.140922579	0.572919145
0.141402292	0.5726293
0.141882227	0.572339842
0.142362384	0.57205077
0.142842763	0.571762085
0.143323363	0.571473788
0.143804184	0.571185878
0.144285225	0.570898355
0.144766487	0.57061122
0.145247969	0.570324473
0.145729671	0.570038114
0.146211593	0.569752144
0.146693733	0.569466562
0.147176093	0.569181368
0.147658671	0.568896563
0.148141467	0.568612148
0.148624481	0.568328121
0.149107713	0.568044484
0.149591163	0.567761236
0.150074829	0.567478378
0.150558713	0.567195909
0.151042812	0.566913831
0.151527128	0.566632143
0.15201166	0.566350845
0.152496408	0.566069938

0.152981371	0.565789422
0.153466549	0.565509296
0.153951941	0.565229562
0.154437548	0.564950218
0.154923369	0.564671267
0.155409404	0.564392706
0.155895653	0.564114538
0.156382114	0.563836761
0.156868789	0.563559377
0.157355676	0.563282384
0.157842776	0.563005785
0.158330087	0.562729577
0.15881761	0.562453763
0.159305345	0.562178341
0.15979329	0.561903313
0.160281447	0.561628678
0.160769814	0.561354436
0.161258391	0.561080588
0.161747178	0.560807134
0.162236175	0.560534074
0.162725381	0.560261408
0.163214796	0.559989136
0.163704419	0.559717259
0.164194251	0.559445776
0.164684291	0.559174688
0.165174539	0.558903996
0.165664994	0.558633698
0.166155657	0.558363796
0.166646526	0.558094289
0.167137602	0.557825177
0.167628884	0.557556462
0.168120372	0.557288142
0.168612066	0.557020219
0.169103965	0.556752692
0.169596069	0.556485561
0.170088378	0.556218827
0.170580892	0.55595249
0.171073609	0.55568655
0.17156653	0.555421007
0.172059655	0.555155861
0.172552983	0.554891113
0.173046514	0.554626763
0.173540248	0.55436281
0.174034184	0.554099255
0.174528321	0.553836098
0.175022661	0.55357334
0.175517202	0.553310979
0.176011944	0.553049018
0.176506887	0.552787455
0.17700203	0.552526292
0.177497373	0.552265527
0.177992917	0.552005161
0.178488659	0.551745195
0.178984601	0.551485629
0.179480742	0.551226462
0.179977082	0.550967695
0.18047362	0.550709329
0.180970356	0.550451362
0.18146729	0.550193796
0.181964421	0.54993663
0.182461749	0.549679865
0.182959274	0.549423501
0.183456995	0.549167538
0.183954913	0.548911976
0.184453026	0.548656815
0.184951335	0.548402056
0.18544984	0.548147698
0.185948539	0.547893743
0.186447433	0.547640189
0.186946521	0.547387037

0.187445803	0.547134288
0.187945279	0.546881941
0.188444948	0.546629996
0.188944811	0.546378454
0.189444866	0.546127316
0.189945113	0.54587658
0.190445553	0.545626247
0.190946185	0.545376318
0.191447008	0.545126792
0.191948022	0.54487767
0.192449228	0.544628952
0.192950624	0.544380638
0.19345221	0.544132727
0.193953986	0.543885221
0.194455952	0.54363812
0.194958108	0.543391423
0.195460452	0.543145131
0.195962985	0.542899244
0.196465707	0.542653761
0.196968616	0.542408684
0.197471714	0.542164013
0.197974999	0.541919746
0.198478471	0.541675886
0.19898213	0.541432431
0.199485976	0.541189382
0.199990008	0.540946739
0.200494226	0.540704503
0.200998629	0.540462673
0.201503218	0.540221249
0.202007992	0.539980232
0.202512951	0.539739622
0.203018094	0.539499419
0.203523421	0.539259623
0.204028932	0.539020235
0.204534626	0.538781254
0.205040504	0.53854268
0.205546564	0.538304514
0.206052807	0.538066756
0.206559232	0.537829406
0.207065839	0.537592464
0.207572627	0.537355931
0.208079597	0.537119806
0.208586748	0.536884089
0.209094079	0.536648782
0.209601591	0.536413883
0.210109282	0.536179393
0.210617154	0.535945313
0.211125205	0.535711642
0.211633434	0.53547838
0.212141843	0.535245528
0.21265043	0.535013085
0.213159195	0.534781053
0.213668138	0.534549431
0.214177259	0.534318219
0.214686556	0.534087417
0.215196031	0.533857025
0.215705682	0.533627045
0.216215509	0.533397475
0.216725513	0.533168316
0.217235691	0.532939568
0.217746046	0.532711231
0.218256575	0.532483305
0.218767279	0.532255791
0.219278157	0.532028689
0.219789209	0.531801998
0.220300435	0.53157572
0.220811834	0.531349853
0.221323407	0.531124399
0.221835152	0.530899356
0.222347069	0.530674727

0.222859159	0.53045051
0.223371421	0.530226705
0.223883854	0.530003314
0.224396458	0.529780335
0.224909233	0.52955777
0.225422179	0.529335618
0.225935295	0.529113879
0.22644858	0.528892554
0.226962036	0.528671642
0.22747566	0.528451145
0.227989454	0.528231061
0.228503416	0.528011392
0.229017547	0.527792136
0.229531846	0.527573295
0.230046312	0.527354869
0.230560946	0.527136857
0.231075747	0.52691926
0.231590714	0.526702078
0.232105848	0.526485311
0.232621148	0.526268959
0.233136614	0.526053023
0.233652245	0.525837502
0.234168042	0.525622396
0.234684003	0.525407706
0.235200129	0.525193432
0.235716419	0.524979574
0.236232873	0.524766133
0.23674949	0.524553107
0.237266271	0.524340498
0.237783214	0.524128305
0.23830032	0.523916529
0.238817589	0.52370517
0.239335019	0.523494227
0.239852611	0.523283702
0.240370364	0.523073594
0.240888279	0.522863903
0.241406354	0.522654629
0.241924589	0.522445773
0.242442984	0.522237335
0.242961539	0.522029315
0.243480254	0.521821712
0.243999127	0.521614528
0.24451816	0.521407761
0.24503735	0.521201413
0.245556699	0.520995484
0.246076206	0.520789973
0.24659587	0.520584881
0.247115691	0.520380207
0.247635669	0.520175953
0.248155804	0.519972118
0.248676095	0.519768701
0.249196541	0.519565705
0.249717143	0.519363127
0.250237901	0.519160969
0.250758813	0.518959231
0.25127988	0.518757913
0.251801101	0.518557015
0.252322476	0.518356537
0.252844005	0.518156479
0.253365687	0.517956841
0.253887522	0.517757624
0.254409509	0.517558827
0.254931649	0.517360451
0.255453941	0.517162496
0.255976384	0.516964962
0.256498979	0.516767849
0.257021725	0.516571157
0.257544622	0.516374886
0.258067669	0.516179037
0.258590866	0.51598361

0.259114212	0.515788604
0.259637709	0.51559402
0.260161354	0.515399857
0.260685148	0.515206117
0.26120909	0.515012799
0.261733181	0.514819903
0.262257419	0.51462743
0.262781805	0.514435379
0.263306338	0.514243751
0.263831018	0.514052545
0.264355844	0.513861763
0.264880816	0.513671403
0.265405935	0.513481466
0.265931199	0.513291953
0.266456608	0.513102863
0.266982162	0.512914197
0.26750786	0.512725954
0.268033703	0.512538134
0.268559689	0.512350739
0.269085819	0.512163767
0.269612093	0.51197722
0.270138509	0.511791096
0.270665068	0.511605397
0.271191769	0.511420123
0.271718612	0.511235272
0.272245597	0.511050847
0.272772723	0.510866846
0.27329999	0.51068327
0.273827397	0.510500119
0.274354945	0.510317393
0.274882633	0.510135092
0.275410461	0.509953216
0.275938428	0.509771766
0.276466534	0.509590741
0.276994778	0.509410142
0.277523161	0.509229969
0.278051682	0.509050221
0.278580341	0.5088709
0.279109137	0.508692004
0.27963807	0.508513535
0.28016714	0.508335492
0.280696346	0.508157876
0.281225689	0.507980686
0.281755167	0.507803922
0.28228478	0.507627585
0.282814529	0.507451676
0.283344412	0.507276193
0.28387443	0.507101137
0.284404582	0.506926508
0.284934868	0.506752307
0.285465287	0.506578532
0.285995839	0.506405186
0.286526524	0.506232267
0.287057341	0.506059776
0.287588291	0.505887712
0.288119373	0.505716077
0.288650585	0.505544869
0.28918193	0.50537409
0.289713404	0.505203738
0.29024501	0.505033816
0.290776745	0.504864321
0.291308611	0.504695255
0.291840606	0.504526618
0.29237273	0.50435841
0.292904983	0.50419063
0.293437364	0.504023279
0.293969874	0.503856358
0.294502511	0.503689865
0.295035276	0.503523802
0.295568169	0.503358168

0.296101188	0.503192964
0.296634334	0.503028189
0.297167606	0.502863844
0.297701003	0.502699929
0.298234527	0.502536444
0.298768175	0.502373388
0.299301949	0.502210763
0.299835847	0.502048568
0.300369869	0.501886803
0.300904015	0.501725469
0.301438285	0.501564565
0.301972678	0.501404091
0.302507194	0.501244049
0.303041833	0.501084437
0.303576594	0.500925256
0.304111476	0.500766506
0.304646481	0.500608187
0.305181606	0.500450299
0.305716853	0.500292842
0.30625222	0.500135817
0.306787708	0.499979224
0.307323315	0.499823062
0.307859042	0.499667331
0.308394888	0.499512032
0.308930853	0.499357166
0.309466937	0.499202731
0.310003139	0.499048728
0.310539459	0.498895157
0.311075897	0.498742019
0.311612452	0.498589313
0.312149124	0.498437039
0.312685913	0.498285198
0.313222818	0.498133789
0.313759838	0.497982813
0.314296975	0.49783227
0.314834227	0.49768216
0.315371593	0.497532483
0.315909075	0.497383239
0.31644667	0.497234428
0.31698438	0.49708605
0.317522203	0.496938106
0.31806014	0.496790595
0.31859819	0.496643517
0.319136352	0.496496874
0.319674626	0.496350664
0.320213013	0.496204887
0.320751511	0.496059545
0.321290121	0.495914637
0.321828841	0.495770163
0.322367672	0.495626123
0.322906614	0.495482517
0.323445665	0.495339345
0.323984826	0.495196608
0.324524096	0.495054306
0.325063476	0.494912438
0.325602964	0.494771005
0.32614256	0.494630006
0.326682264	0.494489443
0.327222076	0.494349314
0.327761996	0.49420962
0.328302022	0.494070362
0.328842155	0.493931539
0.329382394	0.493793151
0.329922739	0.493655198
0.33046319	0.493517681
0.331003746	0.4933806
0.331544407	0.493243954
0.332085173	0.493107744
0.332626043	0.49297197
0.333167017	0.492836631

0.333708095	0.492701729
0.334249275	0.492567262
0.334790559	0.492433232
0.335331946	0.492299638
0.335873435	0.492166648
0.336415026	0.492033759
0.336956718	0.491901474
0.337498512	0.491769626
0.338040407	0.491638215
0.338582402	0.49150724
0.339124498	0.491376702
0.339666693	0.4912466
0.340208988	0.491116936
0.340751383	0.490987709
0.341293876	0.490858919
0.341836468	0.490730566
0.342379159	0.49060265
0.342921947	0.490475172
0.343464833	0.490348131
0.344007816	0.490221528
0.344550896	0.490095362
0.345094073	0.489969634
0.345637346	0.489844344
0.346180715	0.489719492
0.346724179	0.489595077
0.347267739	0.489471101
0.347811394	0.489347562
0.348355143	0.489224462
0.348898987	0.4891018
0.349442924	0.488979576
0.349986955	0.48885779
0.350531079	0.488736443
0.351075296	0.488615535
0.351619606	0.488495065
0.352164008	0.488375034
0.352708502	0.488255441
0.353253087	0.488136287
0.353797764	0.488017572
0.354342532	0.487899297
0.35488739	0.48778146
0.355432338	0.487664062
0.355977376	0.487547103
0.356522504	0.487430584
0.357067721	0.487314504
0.357613027	0.487198864
0.358158421	0.487083662
0.358703903	0.486968901
0.359249474	0.486854579
0.359795132	0.486740696
0.360340877	0.486627254
0.360886709	0.486514251
0.361432627	0.486401688
0.361978632	0.486289565
0.362524722	0.486177882
0.363070898	0.486066664
0.363617159	0.485955837
0.364163505	0.485845475
0.364709935	0.485735553
0.36525645	0.485626071
0.365803048	0.48551703
0.36634973	0.485408429
0.366896495	0.485300269
0.367443342	0.485192549
0.367990273	0.48508527
0.368537285	0.484978432
0.369084379	0.484872035
0.369631554	0.484766078
0.370178811	0.484660563
0.370726148	0.484555489
0.371273566	0.484450855

0.371821064	0.484346663
0.372368641	0.484242912
0.372916298	0.484139603
0.373464034	0.484036735
0.374011849	0.483934308
0.374559742	0.483832323
0.375107714	0.483730779
0.375655763	0.483629677
0.376203889	0.483529016
0.376752092	0.483428797
0.377300372	0.48332902
0.377848729	0.483229685
0.378397161	0.483130792
0.378945669	0.483032341
0.379494253	0.482934332
0.380042911	0.482836765
0.380591645	0.48273964
0.381140452	0.482642957
0.381689334	0.482546717
0.382238289	0.482450918
0.382787317	0.482355563
0.383336418	0.48226065
0.383885592	0.482166179
0.384434839	0.482072151
0.384984157	0.481978565
0.385533547	0.481885422
0.386083008	0.481792722
0.38663254	0.481700465
0.387182143	0.481608651
0.387731816	0.481517279
0.388281559	0.481426351
0.388831371	0.481335865
0.389381253	0.481245823
0.389931203	0.481156224
0.390481222	0.481067068
0.39103131	0.480978355
0.391581465	0.480890085
0.392131687	0.480802259
0.392681977	0.480714877
0.393232334	0.480627937
0.393782757	0.480541442
0.394333247	0.48045539
0.394883802	0.480369781
0.395434423	0.480284616
0.395985109	0.480199895
0.39653586	0.480115618
0.397086675	0.480031785
0.397637554	0.479948395
0.398188497	0.47986545
0.398739504	0.479782948
0.399290573	0.47970089
0.399841706	0.479619277
0.400392901	0.479538108
0.400944158	0.479457383
0.401495476	0.479377102
0.402046857	0.479297265
0.402598298	0.479217873
0.4031498	0.479138925
0.403701362	0.479060422
0.404252984	0.478982363
0.404804666	0.478904749
0.405356408	0.478827579
0.405908208	0.478750854
0.406460067	0.478674574
0.407011985	0.478598738
0.40756396	0.478523347
0.408115993	0.478448401
0.408668084	0.4783739
0.409220231	0.478299844
0.409772435	0.478226232

0.410324695	0.478153066
0.410877011	0.478080345
0.411429383	0.478008069
0.41198181	0.477936238
0.412534292	0.477864852
0.413086829	0.477793911
0.41363942	0.477723416
0.414192065	0.477653366
0.414744763	0.477583761
0.415297514	0.477514602
0.415850319	0.477445888
0.416403176	0.47737762
0.416956085	0.477309798
0.417509046	0.47724242
0.418062058	0.477175489
0.418615122	0.477109003
0.419168237	0.477042963
0.419721401	0.476977368
0.420274617	0.47691222
0.420827881	0.476847517
0.421381196	0.47678326
0.421934559	0.476719449
0.422487972	0.476656084
0.423041432	0.476593165
0.423594941	0.476530692
0.424148498	0.476468665
0.424702101	0.476407084
0.425255752	0.476345949
0.42580945	0.47628526
0.426363194	0.476225018
0.426916984	0.476165222
0.42747082	0.476105872
0.428024701	0.476046968
0.428578627	0.475988511
0.429132598	0.4759305
0.429686613	0.475872936
0.430240672	0.475815818
0.430794775	0.475759146
0.431348921	0.475702921
0.43190311	0.475647143
0.432457342	0.475591811
0.433011616	0.475536926
0.433565932	0.475482488
0.434120289	0.475428496
0.434674688	0.475374951
0.435229127	0.475321853
0.435783607	0.475269201
0.436338128	0.475216997
0.436892688	0.475165239
0.437447288	0.475113928
0.438001927	0.475063065
0.438556604	0.475012648
0.439111321	0.474962678
0.439666075	0.474913155
0.440220867	0.474864079
0.440775697	0.47481545
0.441330564	0.474767269
0.441885467	0.474719534
0.442440407	0.474672247
0.442995383	0.474625407
0.443550395	0.474579014
0.444105443	0.474533069
0.444660525	0.47448757
0.445215642	0.474442519
0.445770793	0.474397916
0.446325979	0.474353759
0.446881198	0.474310051
0.447436451	0.474266789
0.447991736	0.474223975
0.448547055	0.474181609

0.449102405	0.47413969
0.449657788	0.474098219
0.450213202	0.474057195
0.450768647	0.474016618
0.451324124	0.47397649
0.451879631	0.473936809
0.452435168	0.473897575
0.452990735	0.47385879
0.453546332	0.473820452
0.454101958	0.473782562
0.454657613	0.473745119
0.455213297	0.473708124
0.455769008	0.473671578
0.456324748	0.473635479
0.456880515	0.473599827
0.457436309	0.473564624
0.45799213	0.473529869
0.458547978	0.473495561
0.459103851	0.473461701
0.459659751	0.47342829
0.460215676	0.473395326
0.460771626	0.47336281
0.461327601	0.473330743
0.4618836	0.473299123
0.462439623	0.473267952
0.46299567	0.473237228
0.463551741	0.473206953
0.464107834	0.473177125
0.46466395	0.473147746
0.465220089	0.473118815
0.46577625	0.473090332
0.466332432	0.473062298
0.466888635	0.473034711
0.46744486	0.473007573
0.468001105	0.472980883
0.468557371	0.472954641
0.469113656	0.472928848
0.469669961	0.472903503
0.470226286	0.472878606
0.470782629	0.472854157
0.471338991	0.472830157
0.471895371	0.472806605
0.472451769	0.472783502
0.473008184	0.472760846
0.473564617	0.47273864
0.474121067	0.472716881
0.474677533	0.472695571
0.475234015	0.47267471
0.475790513	0.472654297
0.476347027	0.472634332
0.476903556	0.472614816
0.477460099	0.472595748
0.478016657	0.472577129
0.478573229	0.472558958
0.479129815	0.472541236
0.479686414	0.472523963
0.480243027	0.472507137
0.480799652	0.472490761
0.481356289	0.472474833
0.481912939	0.472459353
0.4824696	0.472444322
0.483026273	0.47242974
0.483582956	0.472415606
0.484139651	0.472401921
0.484696355	0.472388685
0.48525307	0.472375897
0.485809794	0.472363558
0.486366528	0.472351667
0.48692327	0.472340225
0.487480021	0.472329232

0.48803678	0.472318687
0.488593548	0.472308591
0.489150323	0.472298944
0.489707105	0.472289745
0.490263893	0.472280995
0.490820689	0.472272694
0.491377491	0.472264841
0.491934298	0.472257437
0.492491111	0.472250482
0.493047929	0.472243976
0.493604752	0.472237918
0.49416158	0.472232309
0.494718411	0.472227148
0.495275247	0.472222437
0.495832086	0.472218174
0.496388927	0.472214359
0.496945772	0.472210994
0.497502619	0.472208077
0.498059468	0.472205609
0.498616319	0.47220359
0.499173172	0.472202019
0.499730025	0.472200897
0.500286879	0.472200224
0.500843733	0.4722
1.527743733	0.6798
1.769843733	0.7226
1.980943733	0.7565
2.184643733	0.7865
2.358843733	0.8103
2.524443733	0.8313
2.689043733	0.8509
2.842143733	0.8679
2.990543733	0.8833
3.135343733	0.8976
3.278443733	0.9108
3.412843733	0.9225
3.546943733	0.9336
3.676243733	0.9437
3.800543733	0.9529
3.926543733	0.9617
4.042743733	0.9694
4.158943733	0.9767
4.271943733	0.9834
4.385343733	0.9898
4.494843733	0.9957
4.600443733	1.0011
4.698243733	1.0058
4.799943733	1.0105
4.897943733	1.0147
4.991743733	1.0186
5.084643733	1.0223
5.170043733	1.0254
5.258343733	1.0286
5.350243733	1.0317
5.430343733	1.0343
5.511043733	1.0367
5.590143733	1.039
5.666043733	1.0411
5.743243733	1.043
5.812843733	1.0448
5.882443733	1.0464
5.954043733	1.048
6.021243733	1.0494
6.084843733	1.0506
6.149043733	1.0519
6.206143733	1.0529
6.266143733	1.0539
6.323943733	1.0548
6.381843733	1.0557
6.434943733	1.0565

6.488943733	1.0572
6.538843733	1.0578
6.587643733	1.0584
6.633143733	1.0589
6.682143733	1.0594
6.727343733	1.0599
6.768743733	1.0603
6.813243733	1.0607
6.855243733	1.061
6.896343733	1.0613
6.934343733	1.0616
6.975443733	1.0619
7.012843733	1.0621
7.048643733	1.0623
7.079543733	1.0625
7.112143733	1.0626
7.142643733	1.0628
7.172343733	1.0629
7.207343733	1.0631
7.234843733	1.0632
7.260843733	1.0633
7.290243733	1.0633
7.315443733	1.0634
7.339343733	1.0635
7.365943733	1.0635
7.389843733	1.0636
7.411743733	1.0636
7.433043733	1.0637
7.454443733	1.0637
7.475943733	1.0637
7.496943733	1.0638
7.514643733	1.0638
7.533843733	1.0638
7.549243733	1.0638
7.567443733	1.0638
7.585843733	1.0639
7.601143733	1.0639
7.617943733	1.0639
7.632943733	1.0639
7.643843733	1.0639
7.658243733	1.0639
7.672843733	1.0639
7.685043733	1.0639
7.698143733	1.0639
7.710343733	1.0639
7.722643733	1.0639
7.732143733	1.0639
7.743243733	1.0639
7.753343733	1.0639
7.761843733	1.0639
7.771343733	1.0639
7.778843733	1.0639
7.788043733	1.0639
7.797343733	1.0639
7.805643733	1.0639
7.813443733	1.0639
7.825543733	1.0639
7.831743733	1.0639
7.839643733	1.0639
7.846943733	1.0639
7.853443733	1.0639
7.862543733	1.0639
7.869543733	1.0639
7.875843733	1.0639
7.882543733	1.0639
7.890743733	1.0639
7.894743733	1.0639
7.901343733	1.0639
7.907143733	1.0639
7.914343733	1.0639

7.919343733	1.0639
7.923743733	1.0639
7.929343733	1.0639
7.935543733	1.0639
7.940943733	1.0639
7.944643733	1.0639
7.949943733	1.0639
7.955343733	1.0639
7.963143733	1.0639
7.966443733	1.0639
7.971643733	1.0639
7.977443733	1.0639
7.980443733	1.0639
7.984843733	1.0639
7.991743733	1.0639
7.994743733	1.0639
7.999543733	1.0639
8.003143733	1.0639
8.007243733	1.0639
8.011443733	1.0639
8.018043733	1.0639
8.020843733	1.0639
8.026043733	1.0639
8.029343733	1.0639
8.030643733	1.0639
8.032043733	1.0639
8.037743733	1.0639
8.040443733	1.0639
8.045443733	1.0639
8.049443733	1.0639
8.051843733	1.0639
8.056343733	1.0639
8.058743733	1.0639
8.063143733	1.0639
8.067143733	1.0639
8.068543733	1.0639
8.070843733	1.0639
8.073243733	1.0639
8.075543733	1.0639
8.078743733	1.0639
8.080943733	1.0639
8.085343733	1.0639
8.088343733	1.0639
8.090143733	1.0639
8.093643733	1.0639
8.096643733	1.0639
8.098943733	1.0639
8.103143733	1.0639
8.103343733	1.0639
8.107643733	1.0639
8.109143733	1.0639
8.112743733	1.0639
8.115543733	1.0639
8.119143733	1.0639
8.118743733	1.0639
8.123543733	1.0639
8.123143733	1.0639
8.130543733	1.0639
8.127643733	1.0639
8.132443733	1.0639
8.135843733	1.0639
8.140043733	1.0639
8.137743733	1.0639
8.143343733	1.0639
8.147943733	1.0639
8.151543733	1.0639
8.153743733	1.0639
8.154743733	1.0639
8.158843733	1.0639
8.160443733	1.0639

8.162643733	1.0639
8.164943733	1.0639
8.166443733	1.0639
8.169343733	1.0639
8.172043733	1.0639
8.175043733	1.0639
8.177143733	1.0639
8.181443733	1.0639
8.177343733	1.0639
8.180243733	1.0639
8.182443733	1.0639
8.187843733	1.0639
8.188843733	1.0639
8.190543733	1.0639
8.195943733	1.0639
8.197643733	1.0639
8.198043733	1.0639
8.200943733	1.0639
8.198843733	1.0639
8.203643733	1.0639
8.205243733	1.0639
8.207643733	1.0639
8.208643733	1.0639
8.211743733	1.0639
8.215843733	1.0639
8.215043733	1.0639
8.215543733	1.0639
8.219243733	1.0639
8.219643733	1.0639
8.223943733	1.0639
8.220743733	1.0639
8.226243733	1.0639
8.230443733	1.0639
8.232943733	1.0639
8.235843733	1.0639
8.237143733	1.0639
8.240143733	1.0639
8.242743733	1.0639
8.243943733	1.0639
8.245243733	1.0639
8.248843733	1.0639
8.247243733	1.0639
8.250943733	1.0639
8.253643733	1.0639
8.257343733	1.0639
8.260543733	1.0639
8.261243733	1.0639
8.262643733	1.0639
8.263943733	1.0639
8.267243733	1.0639
8.268843733	1.0639
8.271643733	1.0639
8.271043733	1.0639
8.275043733	1.0639
8.275843733	1.0639
8.277343733	1.0639
8.278743733	1.0639
8.279043733	1.0639
8.284243733	1.0639
8.286443733	1.0639
8.286743733	1.0639
8.288943733	1.0639
8.291543733	1.0639
8.296243733	1.0639
8.297043733	1.0639
8.298743733	1.0639
8.298243733	1.0639
8.298043733	1.0639
8.300043733	1.0639
8.304043733	1.0639

8.306143733	1.0639
8.307743733	1.0639
8.309743733	1.0639
8.312043733	1.0639
8.312843733	1.0639
8.316343733	1.0639
8.320243733	1.0639
8.321943733	1.0639
8.324043733	1.0639
8.327543733	1.0639
8.327943733	1.0639
8.330843733	1.0639
8.330043733	1.0639
8.331143733	1.0639
8.332143733	1.0639
8.330943733	1.0639
8.334943733	1.0639
8.339143733	1.0639
8.337743733	1.0639
8.340843733	1.0639
8.346043733	1.0639
8.349143733	1.0639
8.349043733	1.0639
8.352643733	1.0639
8.355543733	1.0639
8.358643733	1.0639
8.359743733	1.0639
8.363443733	1.0639
8.364643733	1.0639
8.366543733	1.0639
8.367743733	1.0639
8.369043733	1.0639
8.372043733	1.0639
8.371043733	1.0639
8.374643733	1.0639
8.374243733	1.0639
8.378543733	1.0639
8.378743733	1.0639
8.381743733	1.0639
8.385043733	1.0639
8.386343733	1.0639
8.388943733	1.0639
8.390243733	1.0639
8.393543733	1.0639
8.396043733	1.0639
8.395743733	1.0639
8.400143733	1.0639
8.400443733	1.0639
8.401843733	1.0639
8.405143733	1.0639
8.405343733	1.0639
8.408143733	1.0639
8.407743733	1.0639
8.413543733	1.0639
8.413743733	1.0639
8.420143733	1.0639
8.421043733	1.0639
8.422043733	1.0639
8.424743733	1.0639
8.428743733	1.0639
8.426643733	1.0639
8.433043733	1.0639
8.432243733	1.0639
8.437443733	1.0639
8.441443733	1.0639
8.441943733	1.0639
8.443543733	1.0639
8.445243733	1.0639
8.445643733	1.0639
8.450343733	1.0639

8.449543733	1.0639
8.454743733	1.0639
8.453443733	1.0639
8.461643733	1.0639
8.460343733	1.0639
8.463343733	1.0639
8.463243733	1.0639
8.467343733	1.0639
8.470143733	1.0639
8.470843733	1.0639
8.473143733	1.0639
8.475543733	1.0639
8.477343733	1.0639
8.482043733	1.0639
8.483243733	1.0639
8.486243733	1.0639
8.488043733	1.0639
8.491043733	1.0639
8.493443733	1.0639
8.495343733	1.0639
8.495943733	1.0639
8.500843733	1.0639
8.502643733	1.0639
8.504043733	1.0639
8.507043733	1.0639
8.510843733	1.0639
8.509743733	1.0639
8.515743733	1.0639
8.519443733	1.0639
8.519143733	1.0639
8.522843733	1.0639
8.526643733	1.0639
8.528543733	1.0639
8.528243733	1.0639
8.532443733	1.0639
8.534443733	1.0639
8.536343733	1.0639
8.541343733	1.0639
8.543743733	1.0639
8.544043733	1.0639
8.547743733	1.0639
8.549243733	1.0639
8.553543733	1.0639
8.555643733	1.0639
8.555843733	1.0639
8.559143733	1.0639
8.561643733	1.0639
8.560843733	1.0639
8.563943733	1.0639
8.567243733	1.0639
8.569243733	1.0639
8.570943733	1.0639
8.577043733	1.0639
8.578643733	1.0639
8.581843733	1.0639
8.581043733	1.0639
8.585443733	1.0639
8.586543733	1.0639
8.590343733	1.0639
8.593043733	1.0639
8.594043733	1.0639
8.598043733	1.0639
8.599043733	1.0639
8.603143733	1.0639
8.605843733	1.0639
8.608143733	1.0639
8.610943733	1.0639
8.614943733	1.0639
8.617143733	1.0639
8.618243733	1.0639

8.619943733	1.0639
8.621643733	1.0639
8.624943733	1.0639
8.626743733	1.0639
8.627243733	1.0639
8.633643733	1.0639
8.634143733	1.0639
8.643943733	1.0639
8.645043733	1.0639
8.648543733	1.0639
8.649043733	1.0639
8.654343733	1.0639
8.654843733	1.0639
8.658343733	1.0639
8.661143733	1.0639
8.663043733	1.0639
8.665343733	1.0639
8.668343733	1.0639
8.671143733	1.0639
8.674143733	1.0639
8.676443733	1.0639
8.678943733	1.0639
8.680143733	1.0639
8.683143733	1.0639
8.686543733	1.0639
8.687943733	1.0639
8.690843733	1.0639
8.691543733	1.0639
8.697443733	1.0639
8.699343733	1.0639
8.704043733	1.0639
8.705443733	1.0639
8.708943733	1.0639
8.711443733	1.0639
8.716743733	1.0639
8.718143733	1.0639
8.722243733	1.0639
8.724843733	1.0639
8.725543733	1.0639
8.727543733	1.0639
8.729943733	1.0639
8.732043733	1.0639
8.733843733	1.0639
8.736943733	1.0639
8.737643733	1.0639
8.741343733	1.0639
8.744943733	1.0639
8.748643733	1.0639
8.752243733	1.0639
8.753743733	1.0639
8.757943733	1.0639
8.759443733	1.0639
8.761943733	1.0639
8.765643733	1.0639
8.767043733	1.0639
8.772043733	1.0639
8.772243733	1.0639
8.777143733	1.0639
8.777443733	1.0639
8.780043733	1.0639
8.782543733	1.0639
8.786343733	1.0639
8.788843733	1.0639
8.790943733	1.0639
8.792843733	1.0639
8.798343733	1.0639
8.801443733	1.0639
8.804643733	1.0639
8.808343733	1.0639
8.811043733	1.0639

8.813043733	1.0639
8.816243733	1.0639
8.818243733	1.0639
8.819743733	1.0639
8.821243733	1.0639
8.824543733	1.0639
8.826543733	1.0639
8.837243733	1.0639
8.839243733	1.0639
8.843743733	1.0639
8.846943733	1.0639
8.850243733	1.0639
8.852843733	1.0639
8.855043733	1.0639
8.859343733	1.0639
8.861543733	1.0639
8.863043733	1.0639
8.866343733	1.0639
8.868943733	1.0639
8.873443733	1.0639
8.876643733	1.0639
8.880043733	1.0639
8.883243733	1.0639
8.886643733	1.0639
8.889243733	1.0639
8.890943733	1.0639
8.893543733	1.0639
8.895843733	1.0639
8.897343733	1.0639
8.900743733	1.0639
8.902843733	1.0639
8.906243733	1.0639
8.908943733	1.0639
8.912343733	1.0639
8.915643733	1.0639
8.919043733	1.0639
8.921243733	1.0639
8.925843733	1.0639
8.928543733	1.0639
8.933143733	1.0639
8.935843733	1.0639
8.938743733	1.0639
8.943243733	1.0639
8.944943733	1.0639
8.946643733	1.0639
8.951243733	1.0639
8.954043733	1.0639
8.956943733	1.0639
8.959643733	1.0639
8.963143733	1.0639
8.967143733	1.0639
8.970643733	1.0639
8.972843733	1.0639
8.976343733	1.0639
8.977443733	1.0639
8.980943733	1.0639
8.983143733	1.0639
8.986643733	1.0639
8.986643733	1.0639
8.990143733	1.0639
8.992443733	1.0639
8.995343733	1.0639
8.997043733	1.0639
9.000543733	1.0639
9.001143733	1.0639
9.006943733	1.0639
9.009143733	1.0639
9.012143733	1.0639
9.014943733	1.0639
9.018543733	1.0639

9.020843733	1.0639
9.024343733	1.0639
9.026043733	1.0639
9.029643733	1.0639
9.031943733	1.0639
9.034343733	1.0639
9.036643733	1.0639
9.038443733	1.0639
9.043143733	1.0639
9.043843733	1.0639
9.047943733	1.0639
9.050343733	1.0639
9.054543733	1.0639
9.059443733	1.0639
9.060643733	1.0639
9.065443733	1.0639
9.070643733	1.0639
9.074243733	1.0639
9.077743733	1.0639
9.080243733	1.0639
9.081543733	1.0639
9.087343733	1.0639
9.088043733	1.0639
9.093343733	1.0639
9.096243733	1.0639
9.102743733	1.0639
9.108543733	1.0639
9.108143733	1.0639
9.113343733	1.0639
9.115343733	1.0639
9.117143733	1.0639
9.120243733	1.0639
9.124343733	1.0639
9.128043733	1.0639
9.130943733	1.0639
9.134043733	1.0639
9.137043733	1.0639
9.139543733	1.0639
9.140843733	1.0639
9.145143733	1.0639
9.150343733	1.0639
9.152843733	1.0639
9.156443733	1.0639
9.158943733	1.0639
9.160743733	1.0639
9.165643733	1.0639
9.168643733	1.0639
9.173543733	1.0639
9.177143733	1.0639
9.179743733	1.0639
9.182843733	1.0639
9.185943733	1.0639
9.190743733	1.0639
9.194443733	1.0639
9.196443733	1.0639
9.198943733	1.0639
9.201443733	1.0639
9.203443733	1.0639
9.207043733	1.0639
9.210743733	1.0639
9.213143733	1.0639
9.218143733	1.0639
9.219943733	1.0639
9.222543733	1.0639
9.225043733	1.0639
9.228743733	1.0639
9.229043733	1.0639
9.233343733	1.0639
9.235743733	1.0639
9.238643733	1.0639

9.241043733	1.0639
9.244543733	1.064
9.248143733	1.064
9.252843733	1.064
9.254643733	1.064
9.259843733	1.064
9.261143733	1.064
9.263043733	1.064
9.268343733	1.064
9.270843733	1.064
9.273343733	1.064
9.277443733	1.064
9.281643733	1.064
9.283543733	1.064
9.286043733	1.064
9.288443733	1.064
9.292043733	1.064
9.295043733	1.064
9.296943733	1.064
9.302243733	1.064
9.305843733	1.064
9.307643733	1.064
9.312943733	1.064
9.314843733	1.064
9.321343733	1.064
9.323143733	1.064
9.329643733	1.064
9.331543733	1.064
9.335243733	1.064
9.338843733	1.064
9.342543733	1.064
9.344443733	1.064
9.348143733	1.064
9.349543733	1.064
9.353243733	1.064
9.358043733	1.064
9.362343733	1.064
9.366543733	1.064
9.368543733	1.064
9.372743733	1.064
9.375943733	1.064
9.379043733	1.064
9.382143733	1.064
9.385843733	1.064
9.388943733	1.064
9.390943733	1.064
9.395843733	1.064
9.400143733	1.064
9.403243733	1.064
9.405243733	1.064
9.409543733	1.064
9.413843733	1.064
9.415943733	1.064
9.420843733	1.064
9.422343733	1.064
9.427243733	1.064
9.428743733	1.064
9.433643733	1.064
9.436843733	1.064
9.440043733	1.064
9.443243733	1.064
9.448643733	1.064
9.450143733	1.064
9.453343733	1.064
9.457643733	1.064
9.462043733	1.064
9.463543733	1.064
9.467343733	1.064
9.471743733	1.064
9.474443733	1.064

9.478343733	1.064
9.481043733	1.064
9.483643733	1.064
9.491443733	1.064
9.494043733	1.064
9.495643733	1.064
9.500043733	1.064
9.502643733	1.064
9.508143733	1.064
9.510743733	1.064
9.515443733	1.064
9.518243733	1.064
9.524343733	1.064
9.526443733	1.064
9.530243733	1.064
9.532943733	1.064
9.536743733	1.064
9.540543733	1.064
9.543243733	1.064
9.547043733	1.064
9.550343733	1.064
9.553043733	1.064
9.556843733	1.064
9.559543733	1.064
9.565643733	1.064
9.568343733	1.064
9.570943733	1.064
9.572643733	1.064
9.576443733	1.064
9.579143733	1.064
9.583043733	1.064
9.586243733	1.064
9.590743733	1.064
9.596843733	1.064
9.599543733	1.064
9.605043733	1.064
9.610043733	1.064
9.611143733	1.064
9.616643733	1.064
9.618843733	1.064
9.623343733	1.064
9.627243733	1.0641
9.628243733	1.0641
9.634943733	1.0641
9.641643733	1.0641
9.646143733	1.0641
9.651643733	1.0641
9.653943733	1.0641
9.656043733	1.0641
9.660543733	1.0641
9.663843733	1.0641
9.666143733	1.0641
9.669443733	1.0641
9.672743733	1.0641
9.674943733	1.0641
9.679343733	1.0641
9.682743733	1.0641
9.686043733	1.0641
9.689343733	1.0641
9.692643733	1.0641
9.697143733	1.0641
9.699343733	1.0641
9.702643733	1.0641
9.707743733	1.0641
9.711043733	1.0641
9.716643733	1.0641
9.717743733	1.0641
9.722243733	1.0641
9.724443733	1.0641
9.727743733	1.0641

9.729943733	1.0641
9.734443733	1.0641
9.740643733	1.0641
9.741743733	1.0641
9.750243733	1.0641
9.756343733	1.0641
9.760943733	1.0641
9.764243733	1.0641
9.767643733	1.0641
9.773743733	1.0641
9.777143733	1.0641
9.783243733	1.0641
9.786643733	1.0641
9.791743733	1.0641
9.795143733	1.0641
9.800243733	1.0641
9.802443733	1.0641
9.806343733	1.0641
9.809743733	1.0641
9.813043733	1.0641
9.815243733	1.0641
9.818643733	1.0641
9.823643733	1.0641
9.827643733	1.0641
9.831543733	1.0641
9.835543733	1.0641
9.838343733	1.0641
9.842243733	1.0641
9.845043733	1.0641
9.850043733	1.0641
9.852843733	1.0641
9.855043733	1.0641
9.859043733	1.0641
9.861243733	1.0641
9.865143733	1.0641
9.870343733	1.0641
9.873143733	1.0641
9.875943733	1.0641
9.878643733	1.0641
9.883843733	1.0641
9.889443733	1.0641
9.892243733	1.0641
9.897843733	1.0641
9.903443733	1.0641
9.905143733	1.0641
9.910843733	1.0641
9.916443733	1.0641
9.922043733	1.0641
9.923243733	1.0641
9.928843733	1.0641
9.933343733	1.0641
9.936143733	1.0641
9.940743733	1.0641
9.944643733	1.0641
9.948643733	1.0641
9.953243733	1.0641
9.956043733	1.0641
9.960543733	1.0641
9.962343733	1.0641
9.966843733	1.0641
9.971443733	1.0641
9.975943733	1.0641
9.982243733	1.0641
9.985043733	1.0641
9.989543733	1.0641
9.992343733	1.0641
9.995743733	1.0641
9.999143733	1.0641
10.00094373	1.0641
10.00544373	1.0641

10.00824373	1.0641
10.01624373	1.0641
10.01904373	1.0641
10.02364373	1.0641
10.02984373	1.0641
10.03154373	1.0641
10.03434373	1.0641
10.03894373	1.0641
10.04454373	1.0641
10.04634373	1.0641
10.04914373	1.0641
10.05364373	1.0641
10.05654373	1.0641
10.06164373	1.0641
10.06504373	1.0641
10.06844373	1.0641
10.07184373	1.0641
10.07694373	1.0641
10.07984373	1.0641
10.08434373	1.0641
10.08774373	1.0641
10.09234373	1.0641
10.09744373	1.0641
10.10264373	1.0641
10.10604373	1.0641
10.10884373	1.0641
10.11344373	1.0641
10.12014373	1.0641
10.12304373	1.0641
10.12584373	1.0641
10.12924373	1.0641
10.13434373	1.0641
10.13774373	1.0642
10.14114373	1.0642
10.14794373	1.0642
10.15024373	1.0642
10.15704373	1.0642
10.15944373	1.0642
10.16514373	1.0642
10.16744373	1.0642
10.17264373	1.0642
10.17654373	1.0642
10.17894373	1.0642
10.18464373	1.0642
10.18804373	1.0642
10.19544373	1.0642
10.19774373	1.0642
10.20004373	1.0642
10.20524373	1.0642
10.20864373	1.0642
10.21204373	1.0642
10.21544373	1.0642
10.21884373	1.0642
10.22274373	1.0642
10.22674373	1.0642
10.23014373	1.0642
10.23634373	1.0642
10.23864373	1.0642
10.24204373	1.0642
10.24604373	1.0642
10.25174373	1.0642
10.25354373	1.0642
10.25924373	1.0642
10.26324373	1.0642
10.26714373	1.0642
10.27174373	1.0642
10.27574373	1.0642
10.27964373	1.0642
10.28364373	1.0642
10.28934373	1.0642

10.29334373	1.0642
10.29734373	1.0642
10.30064373	1.0642
10.30404373	1.0642
10.30984373	1.0642
10.31374373	1.0642
10.31784373	1.0642
10.32194373	1.0642
10.32764373	1.0642
10.33214373	1.0642
10.33624373	1.0642
10.34074373	1.0642
10.34704373	1.0642
10.34934373	1.0642
10.35344373	1.0642
10.35804373	1.0642
10.36204373	1.0642
10.36434373	1.0642
10.37064373	1.0642
10.37354373	1.0642
10.37984373	1.0642
10.38614373	1.0642
10.39124373	1.0642
10.39814373	1.0642
10.40224373	1.0642
10.40624373	1.0642
10.41084373	1.0642
10.41484373	1.0642
10.41894373	1.0642
10.42294373	1.0642
10.42804373	1.0642
10.43264373	1.0642
10.43664373	1.0642
10.44074373	1.0642
10.44704373	1.0642
10.45104373	1.0642
10.45394373	1.0642
10.45904373	1.0642
10.46364373	1.0642
10.46644373	1.0642
10.46934373	1.0642
10.47624373	1.0642
10.48074373	1.0642
10.48484373	1.0642
10.48884373	1.0642
10.49174373	1.0642
10.49404373	1.0642
10.49974373	1.0642
10.50424373	1.0642
10.50934373	1.0642
10.51284373	1.0642
10.51624373	1.0642
10.51974373	1.0642
10.52484373	1.0642
10.52934373	1.0642
10.53284373	1.0642
10.53564373	1.0642
10.54134373	1.0642
10.54424373	1.0642
10.55164373	1.0642
10.55674373	1.0642
10.56184373	1.0642
10.56634373	1.0642
10.57084373	1.0642
10.57594373	1.0642
10.57884373	1.0642
10.58224373	1.0642
10.59024373	1.0642
10.59304373	1.0642
10.59594373	1.0642

10.60154373	1.0642
10.60664373	1.0642
10.60954373	1.0642
10.61744373	1.0642
10.62084373	1.0642
10.62374373	1.0642
10.63164373	1.0642
10.63504373	1.0642
10.63854373	1.0642
10.64474373	1.0642
10.64984373	1.0642
10.65494373	1.0642
10.65774373	1.0642
10.66064373	1.0642
10.66514373	1.0642
10.66854373	1.0642
10.67594373	1.0642
10.68274373	1.0642
10.68564373	1.0642
10.69024373	1.0642
10.69584373	1.0642
10.69994373	1.0642
10.70394373	1.0642
10.70894373	1.0642
10.71294373	1.0642
10.71584373	1.0642
10.72264373	1.0642
10.72824373	1.0642
10.73174373	1.0642
10.73574373	1.0642
10.74134373	1.0642
10.74364373	1.0642
10.74704373	1.0642
10.75204373	1.0642
10.75604373	1.0642
10.76004373	1.0642
10.76514373	1.0642
10.76854373	1.0642
10.77704373	1.0642
10.78044373	1.0642
10.78544373	1.0642
10.78944373	1.0642
10.79514373	1.0642
10.80014373	1.0642